Correlation Between 90^{o} Tensile and 90^{o} Flexural Properties for Thermoplastic Based Carbon-Fiber Composites

Amy Lautenbach

Advisor: Prof. Blair London

Industry Sponsors: TenCate Advanced Composites and The Boeing Company

Approval Page

Project Title: CORRELATION BETWEEN 90^{o} TENSILE AND 90^{o} FLEXURAL PROPERTIES FOR THERMOPLASTIC BASED CARBON-FIBER COMPOSITES

Author: Amy Lautenbach

Date Submitted: May 31, 2012

CAL POLY STATE UNIVERSITY

Materials Engineering Department

Prof. Blair London _____

Faculty Advisor Signature

Prof. Trevor Harding _____

Department Chair Signature

Abstract

Thermoplastic matrix composites containing carbon fibers and 4 different resins (TP 1-TP 4) were tested in tension with the fibers at 90 degree to the longitudinal axis following ASTM D 3039-00. The tensile strengths varied from 5.07-13.87 ksi with TP 1 as the strongest, and TP 4 as the weakest. SEM images were taken of the fracture surface of the samples to explore the fiber-matrix interaction. The SEM images showed significantly more wetting of the fibers in the higher strength materials. The SEM images of the two stronger materials showed resin coating the fibers even after fracture while the two weaker materials showed a clean interface between the fibers and resin. As the second portion of the project, 3 and 4 point bend tests were conducted on the same 4 composite materials with a support span width of 1.4 inches according to ASTM D 790-03 and ASTM D 6272-02. The fibers were oriented 90 degrees to the long axis of the samples. The 3 point bend test flexural strength values ranged from 8.30-21.73 ksi and the 4 point values ranged from 6.26-19.25 ksi. The only discrepancy with the data points was TP 1 was not consistently stronger than TP 2. Data analysis was run using the STAT17 program to confirm that the TP 1 and TP 2 strength values were comparable and thus the inconsistency was not relevant. The flexural strength values were graphed versus the tensile strength values and showed a strong correlation. The 3 point binding strength versus tensile strength graph had an R^2 value of 0.9894 and the corresponding 4 point binding versus tensile graph had an R^2 value of 0.9979.

keywords: materials engineering, thermoplastic composites, flexural stress, tensile stress, carbon fiber composites

Table of Contents

List of Figures

List of Tables

Acknowledgements:

I would like to first acknowledge Cal Poly State University for the use of their equipment and the education they have provided me. I would like to especially thank Professor Blair London for being my advisor on this project and helping keep me on track throughout the entire process. He was always willing to help and provide constructive criticism during this project. I would like to thank my materials engineering classmates, Nash Anderson and Rishi Kripalani for assistance with gold sputtering as well as imaging on the SEM. I would also like to thank The Boeing Company for providing a structure in addition to funding for my project. To add to this, Aaron Bartel, John Mosher, and Bob Weiss deserve thanks for playing important roles in the structuring and initial design of my project. I would like to thank Michael Larson personally for being my contact at Boeing throughout these 8 months and attending weekly conference calls to answer any questions I may have. TenCate Advanced Materials also played a role in the structure and design of my project and I would like to thank them for their participation and donations as well. Erinann Corrigan, Barry Meyers, Scott Unger, and Jim Mondo were all a part of the team who thought up my problem statement and output expectations. Dan Leeser provided me with the laminates and was my TenCate contact for the entire project who also attended the weekly conference calls. All of these people and many more are the reason I was able to complete this successful senior design project.

Introduction:

The basis of this project comes from The Boeing Company's (Seattle, WA) interest in learning more about the internal fiber-matrix interactions of the thermoplastic based composites they are using for numerous airplane components. This project was also in collaboration with Boeing's main supplier of thermoplastic composites, TenCate Advanced Materials (Morgan Hill, CA). TenCate hopes that in the near future they will be able to move from qualifying composite materials based on tensile tests to qualifying them based on flexural tests. Flexural testing increases the probability that the sample will fracture at a predetermined point rather than being subject to fail at any given defect in a rather long gage length. Flexural tests would also save significant time and money in the qualification process because they require smaller samples and do not require tabs to be added. The materials used in this project will be carbon fiber reinforced thermoplastic composites with one of four variable thermoplastic resins and a 60% fiber volume fraction.

The first part of this project will be performing flexural and 90 degree tension tests on the composites to prove the correlation between the two tests and validate TenCate's use of flexural testing in place of tensile testing. The second part of this project will look further into the structure of the composite with scanning electron microscope (SEM) images and photo micrographs of the fracture surface. These images will be taken to explore the fiber-matrix interactions within each of these materials after they have been fractured. They will be used to demonstrate which of the resin systems creates the strongest bond with the carbon fibers. After this project is completed, Boeing will have a better understanding of the fiber-matrix interfaces inside the composites they are using and TenCate will have a starting point for their transition to flexural testing.

Use of Composites in Aerospace

In the late 1960s and early 1970s fiber-reinforced composites were introduced to the primary structure of commercial and military airplanes. It started with boron fiber-reinforced epoxy skins being

used in the F-14 horizontal stabilizers and quickly led to carbon fiber-reinforced epoxy becoming the main material in wing, empennage, and fuselage components. The use of composites in aerospace increased quickly because of the significant reduction in weight without loss of mechanical strength and durability. Boeing used fiber-reinforced composites in the 737 commercial aircraft which reduced the horizontal stabilizer weight by 22% and the wing spoiler weight by 37% [(1)]. The Boeing Company is the world's largest aerospace company and produces the most commercial jetliners and military aircrafts combined. They have recently been using composites to reduce the weight of their airplanes to make them more cost and fuel efficient. The Boeing 787 Dreamliner is the most recent of their commercial airplanes and is composed of 50% fiber-reinforced composites which saves enough weight to reduce fuel costs by 20% compared to aluminum based commercial airplanes of its size (**Figure 1**). Another reason for using composites in this airplane is the reduced maintenance costs observed in the Boeing 777. The 777's composite tail is 25% larger than the 767's aluminum tail, but the 767's tail requires 35% more maintenance labor hours. The 787 also has less predicted non-routine maintenance hours because of the corrosion reduction provided by increased composite usage as well as titanium alloys [(2)].

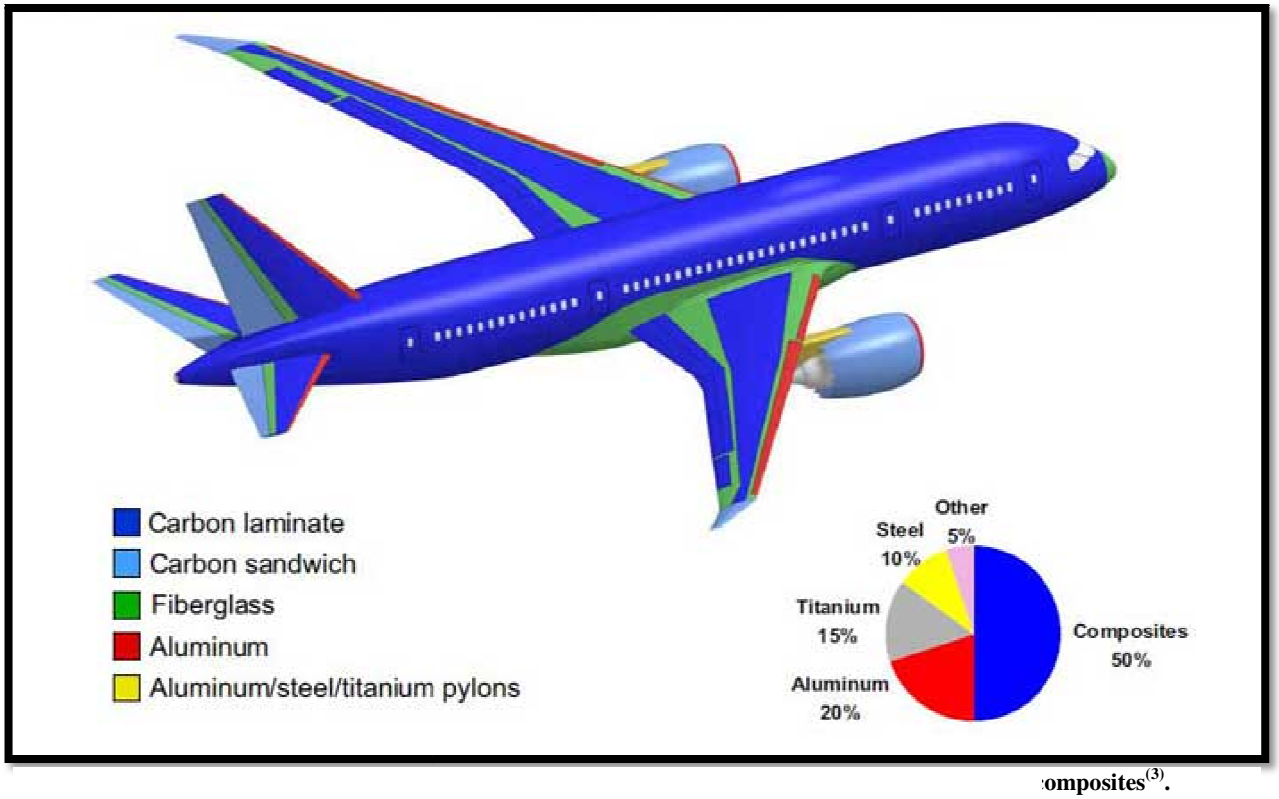

omposites[3].

Thermoplastic composites have thus far been used only in the secondary structure, but Boeing has an interest in exploring different and increased applications [3]. The use of thermoplastic composites will be more cost efficient for mass production of airplanes because of their efficient cycle time and their recyclability. Unlike thermosets, thermoplastic matrices do not cure during their production cycle and therefore processing can be reversed and repeated. One of the main thermoplastic composites in use by the company today is a PEEK based thermoplastic composite reinforced with carbon fibers and produced by TenCate.

Carbon Fiber Use in Industry

In recent years, carbon fibers have been widely used as high-strength materials but also to improve the strength of composite materials. In 1879 Thomas Edison was the first to use carbon fiber and took out a patent to manufacture carbon filaments for his electric lamps. It was not until the early 1960s,

however, that carbon fibers were produced commercially and used in the aircraft industry. Carbon fibers are used to reinforce composites when high strength, stiffness, and low weight are all important requirements. They are also useful in the aerospace industry because of their high temperature resistance, chemical inertness, and high damping [4].

Although carbon-fiber reinforced materials are up to five times the cost of glass-fiber reinforced thermoplastics they offer substantially higher ultimate tensile strengths and stiffness. Glass-reinforced composites have carbon contents as low as 10% and have a higher coefficient of expansion and mold shrinkage. The carbon-fiber reinforcement in plastic also adds conductivity which reduces static charges and therefore is useful in aerospace applications [5]. In processing these carbon fibers, polyacrylonitrile (PAN) is the most commonly used precursor. Processing at higher temperatures produces a graphite fiber which has a higher elastic modulus but lower elongation and ultimate strength, which is not ideal for aerospace applications. The alternative method for processing carbon fibers is based on pitch as a precursor. Pitch is relatively inexpensive and is made of an isotropic mixture of largely aromatic compounds. If the pitch is converted into a mesophase before processing is complete, a high strength and high modulus fiber can be produced. The carbon content obtained from this process can reach up to 80% while PAN fiber processing reaches only 50% [6]. Since carbon fibers can be processed with various precursors, their mechanical properties vary as well. The mechanical properties of these fibers are also determined by the processing conditions, heat treatment temperature, and the existence of flaws or defects[4].

Fiber Orientation

Fiber orientation can have a substantial impact on the mechanical properties of a composite and therefore must always be considered when analyzing composites. This report will be focusing on unidirectional, 90 degree orientation of fibers in composites. This means that the fibers lay unidirectional and perpendicular to the length of the testing bars. This is important to take into consideration because

the direction of fibers affects the properties of the material in each direction. Unidirectional fiber composites have the highest strength and modulus in the direction of the fiber axis [6]. This means that during tensile testing the composites are being monotonically loaded perpendicular to the direction of the fibers (**Figure 2**).

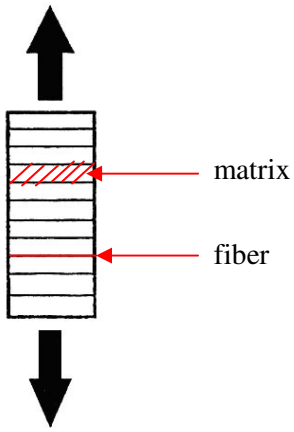

Figure 2: The monotonic loading of the composite sample in a tensile test with the fiber perpendicular to the tensile axis.

In a study done by S. Solaimurugan and R. Velmurugan it was verified that the direction of fibers in the composite also impacts the propagation of cracks in the matrix. In homogeneous polymer materials, cracks can propagate in any direction but when there are fibers embedded in the matrix they guide the crack propagation. They also discovered that as the orientation angle of the fiber increased with respect to the matrix, the fracture toughness increased. It was reported to have nearly doubled as crack direction and fiber orientation angle increased from 0 to 90 degrees [7].

Thermoplastic Matrices

Thermosets are used more often than thermoplastics because of their high-temperature strength and resistance to solvents. Although thermosets are superior in high temperature applications, thermoplastics are recyclable. This efficiency in processing makes them preferred if the properties are sufficient for the application and, as processing technology evolves, thermoplastics are more frequently

replacing thermosets. Thermoplastics are completely recyclable because there is no curing involved in their processing and so they can be reprocessed without losing any of their properties. In mass production of airplanes, this is more resourceful for processing than that of thermosets. The processing of thermoplastic also produces no volatile organic compounds and the products are completely resistant to aircraft fluids. Thermoplastics do not require refrigeration, bagging, time for curing, or disposal after a certain amount of months of not being used. These matrices also reduce flammability, and smoke and toxicity risks which are all important for the interior of an aircraft. Unfortunately however, they are not resistant to UV radiation, concentrated nitric acid, general acid-oxidizing conditions, and therefore cannot yet be used in primary structural components of the airplane [6].

In industry today there are four types of thermoplastic matrices being used; polyether ether ketone (PEEK), polyetherketoneketone (PEKK), polyphenylene sulphide (PPS), and polyether imide (PEI). **Table I** shows a comparison of the tensile and flexural strengths of these materials assuming 30% carbon fiber fraction by weight.

Table I: Comparison of Tensile and Flexural Strength Values for Various Matrices

	PEEK	PEI	PEKK	PPS
Tensile Strength (ksi)	27.6-33.1	29.0-33.9	27.4-30.3	20.0-27.0
Flexural Strength (ksi)	40.0-48.6	37.0-45.0	34.2-37.8	26.0-36.0

Table I shows PEEK as having the highest potential flexural strength and PEI having the highest potential tensile strength. PEKK appears to have average strength values and PPS has the lowest flexural and tensile strengths.

Flexural Properties: 3 and 4 Point Bend Testing

Flexural testing uses 3 and 4 point loading on a beam to bend the sample to its maximum fiber stress while the stress and strain are recorded. Once complete, the test produces a stress-strain diagram to show the progression of material weakening over given loads. The slope of this line is also used to find

the flexural modulus. When the beam is in loading, tensile stress is created on the convex side of the beam and compression stress is created on the concave side. The span to depth ratio is controlled to minimize the shear stress produced along the center of the beam. The primary difference between 3 and 4-point flexural tests is the size of the area of uniform stress. In a 3-point bend test the stress is concentrated under the center loading point while the 4-point bend tests allows for the uniform stress to be spread throughout the area between the two center loading points (**Figure 3 and 4**) [8].

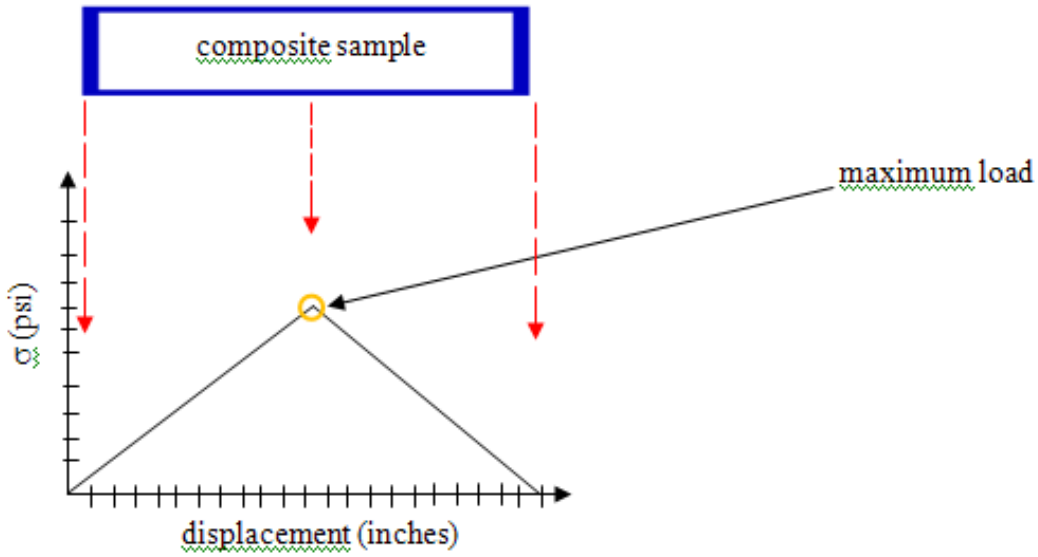

Figure 3: Distribution of the load over the composite sample in 3 point bend testing.

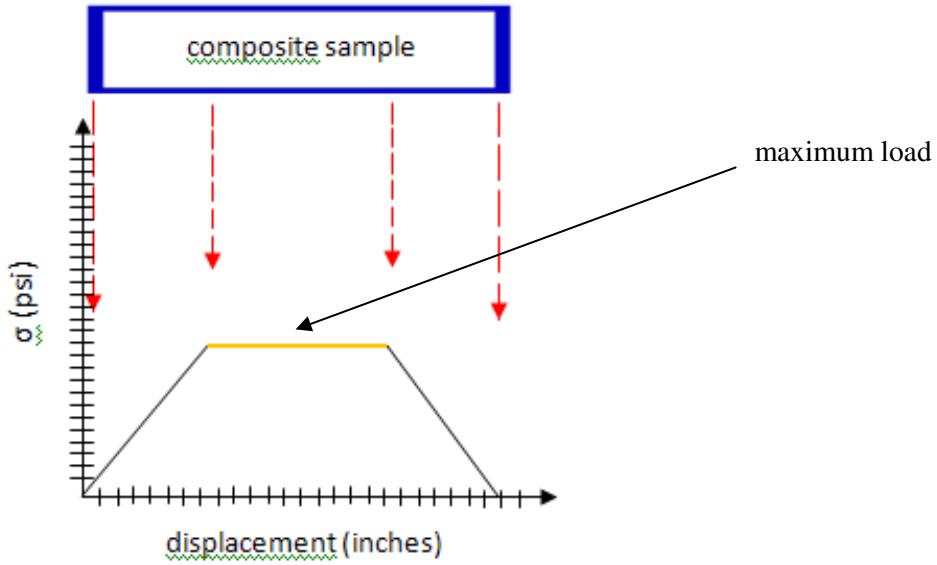

Figure 4: Distribution of the load over the composite sample for 4 point bend testing.

Figure 3 gives a visual representation of the concentrated load applied to the composite sample during a 3 point bend test. **Figure 4** shows the distribution of the load over the center of the composite sample because of the two loading noses used in 4 point bend testing. The lack of distribution of load in 3 point bend testing assures that the sample will break in a certain spot. The distribution of load seen in 4 point bend testing allows for a more accurate representation of the entire sample's properties. If there is a flaw in the composite where the 3 point loading nose is positioned the test may not give an accurate representation of the properties of the mass material.

90 Degree Tensile Testing

Cambridge Engineering Selector (CES) defines ultimate tensile strength as, "the maximum engineering stress in a uniaxial stress-strain test [(9)]." It is calculated by dividing the applied load by the cross-sectional area of the specimen and is used for qualification of composites in industry. In the case of composites, the tensile strength is slightly higher than the yield strength because the load is

transferred to the reinforcing fibers before ultimate fracture [9]. The maximum load in tensile testing is ideally subject to the middle of the sample where necking occurs (**Figure 5**).

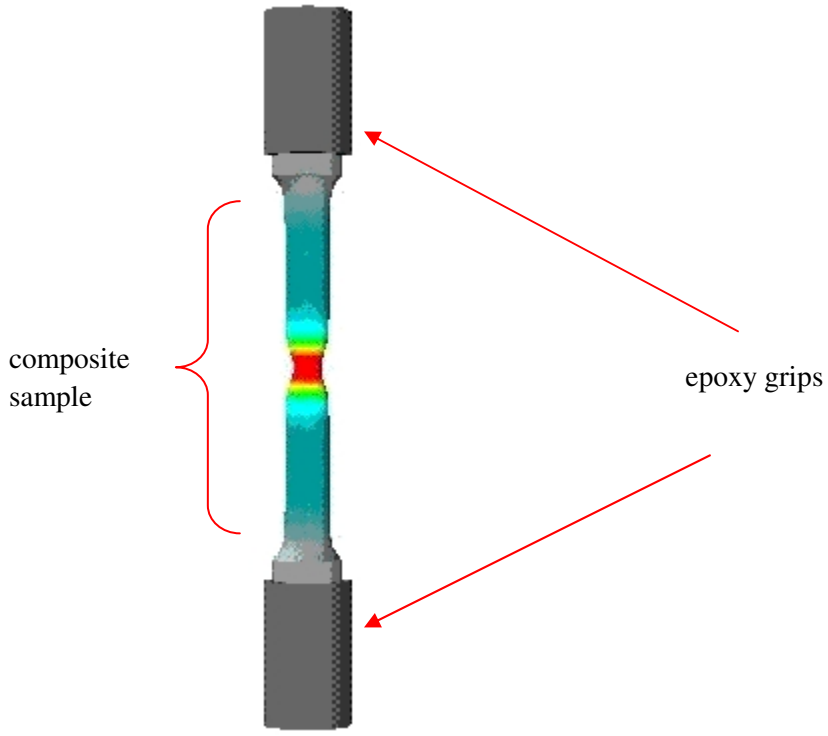

Figure 5: Visual representation of the force distribution of a sample in tension[10].

The most difficult component of axial loading of a unidirectional composite is figuring out how to grip the composite specimen without introducing new stress concentrations. This is the reason for introducing grips on the end of the composite samples that will transfer the applied tensile force through shear stress at the specimen surface into tensile stresses within the specimen. Using softer grips that are adhered to the specimen can help minimize these clamping forces [11].

Imaging of Fiber-Matrix Interface

Microscopy of composites is more complicated than typical metallography because of the hardness of the fibers and the softness of the matrix. Composites can be mounted in materials such as polyester, acrylic, or epoxy resin with epoxy being the preferable mounting material. Epoxy is preferable

because it has the least shrinking during curing to eliminate movement of the sample during curing. The samples are mounted and cured in the epoxy at room temperature for at least 8 hours. Microscopy of composites can be used for analysis of the fiber volume fraction as well as detecting voids in the material. It can also be used to observe the composite as a whole and to gain information on the bonding between the fiber and matrix. Imaging the cross-section of a composite illustrates different information depending on the fiber orientation (**Figure 6**) [12]. If the fibers are oriented in the 90 degree direction more information can be obtained about the fiber volume fraction rather than fibers oriented at 0 degrees which show more of the fiber-matrix bond.

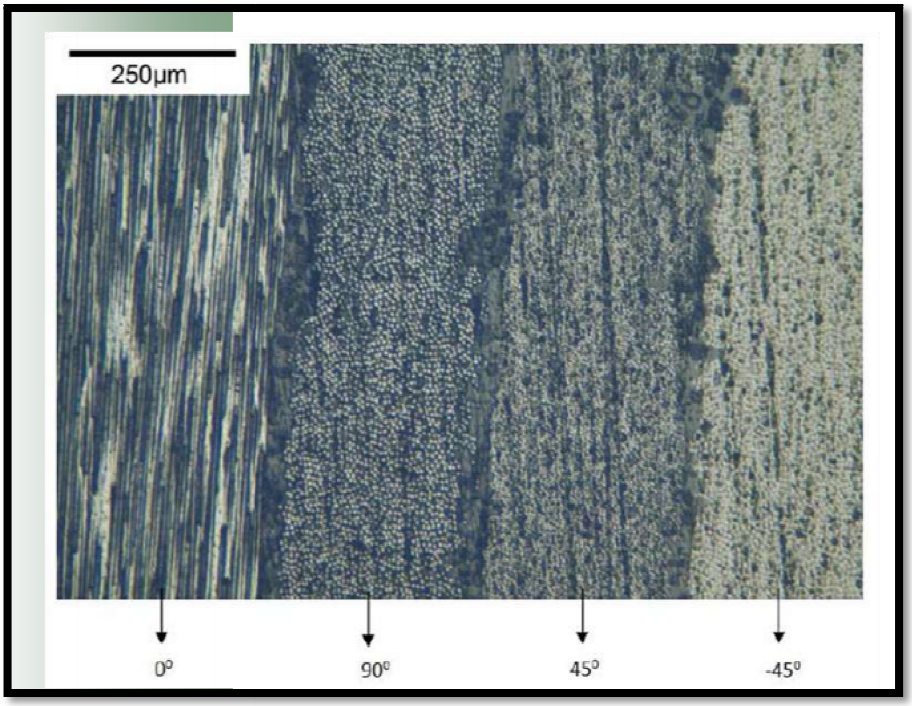

Figure 6: A visual representation of the cross-sections of different composites depending on fiber orientation.

While microscopy of composites provides sufficient magnification for basic fiber-matrix interactions, SEM imaging is preferred for a more in depth analysis. SEM provides much higher magnifications as well as a greater depth of field. This imaging allows for analysis of interaction between individual fibers and their surrounding resin (**Figure 7**) [12].

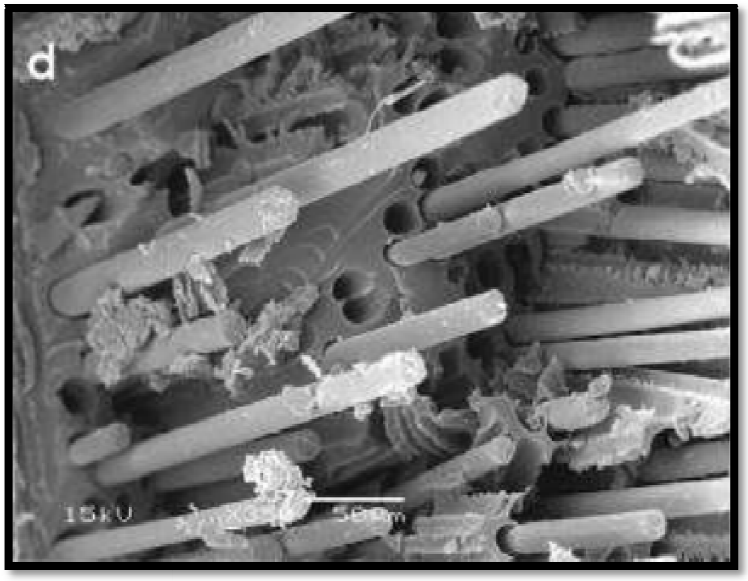

Figure 7: An SEM image of a composite that shows individual fiber-matrix interactions.

In a composite with a 90 degree fiber orientation SEM imaging could be used to analyze the fiber-matrix interaction on the fracture surface. Microscopy of the same composite would provide information on the resin distribution and presence of cracks [(12)].

Realistic Constraints [(13)]

The carbon fiber reinforced thermoplastic composites analyzed in this project are used by Boeing in various aircraft components. The two realistic constraints that relate to my project are economic and sustainability. The significant weight loss provided by the use of composites reduces the amount of fuel it takes to fly the aircraft and therefore reduces the economic cost of flights. The reduction in economic cost of each flight will in turn reduce the cost of travel. The decrease in corrosion that also stems directly from the replacement of aluminum with composites allows for a longer life cycle of each airplane thus making them more sustainable. Using thermoplastic composites instead of thermoset composites will also increase the recyclability of airplane parts after the airplane's lifecycle.

Experimental Procedure:

Materials Provided

For this project, TenCate provided 68 carbon fiber reinforced thermoplastic composite samples with 4 varying thermoplastic resins (TP1-TP4) for mechanical testing (**Table II**). The samples were then divided into their respective groups and labeled on both top and bottom so they would still be identifiable after the fracture.

Table II: Test Matrix of Composite Samples

Material	Tensile test samples (5 in. x 1 in x 0.09 in)	3 point bend test samples (2.5 in. x 0.5 in. x 0.09 in.)	4 point bend test samples (2.5 in. x 0.5 in. x 0.09 in.)
TP 1	6	6	5
TP 2	6	6	5
TP 3	6	6	5
TP 4	6	6	5

Tensile Testing

The tensile testing was conducted according to ASTM D 3039/D 3039M [(14)]. This test method involves a thin rectangular sample with a constant rectangular cross section to be gripped vertically in the mechanical testing machine. The sample is then monotonically loaded at a constant rate, in tension, and the load is recorded in desired time increments until the material reaches its ultimate tensile strength and fractures. The data collected from this test will provide a load versus displacement plot and ultimately give tensile stresses that will be correlated with the flexural stresses of the 3 and 4 point bend tests [(14)].

For the tensile test, 6 rectangular coupons of 5 inches by 1 inch by 0.09 inches were provided for each of the 4 materials with grip tabs attached. The tensile testing was completed with these samples placed vertically in the Instron 3369 tensile testing system (**Figure 8**) using an 11,000 lb load cell. The cross head speed recommended by the standard and used for this test was 0.05 inches per minute [14]. These samples were then monotonically loaded in tension moving at this crosshead speed while the load was recorded.

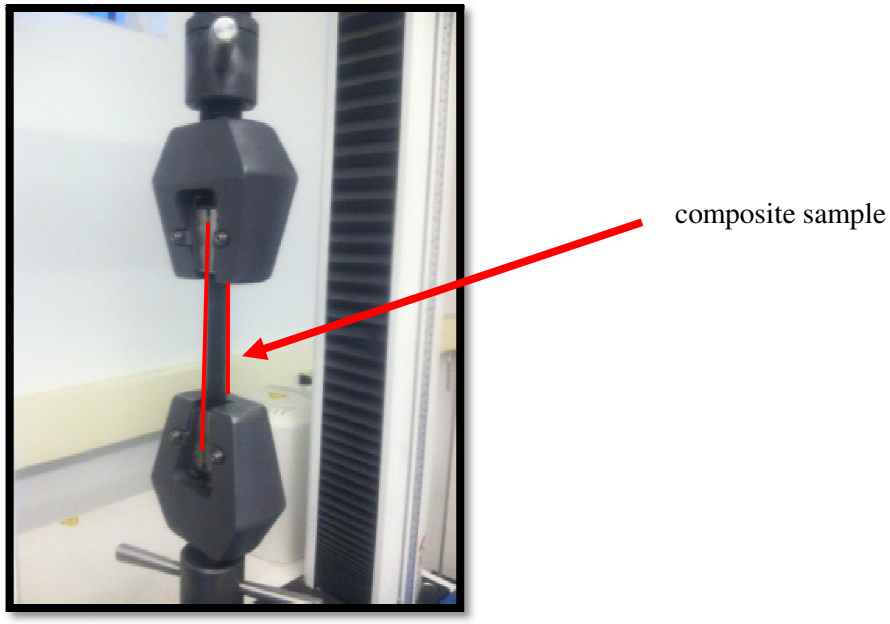

Figure 8: A composite sample loaded vertically in the Instron 3369 tensile testing system with the tabs secure in the grips and the remainder of the composite sample exposed.

3 and 4 Point Bend Testing

The 3 point flexural bend test was conducted according to ASTM D 790-03 [8]. The 16:1 support span-to-depth ratio for 3 point flexural testing recommended by the standard was used. For the samples in this test the depth is 0.09 inches therefore putting the support span at 1.44 inches. **Figures 9** gives a visual of the support span measurement and 3 point bend test set up. For 3 point bend testing the equation for crosshead displacement rate for materials that break at comparatively small deflections is:

$$R = 0.167ZL^2/d \quad (1)$$

Where Z is equal to 0.01, L is equal to the support span, and d is equal to the depth of the beam which [16]. The rate of crosshead motion was calculated to be 0.038 inches per minute.

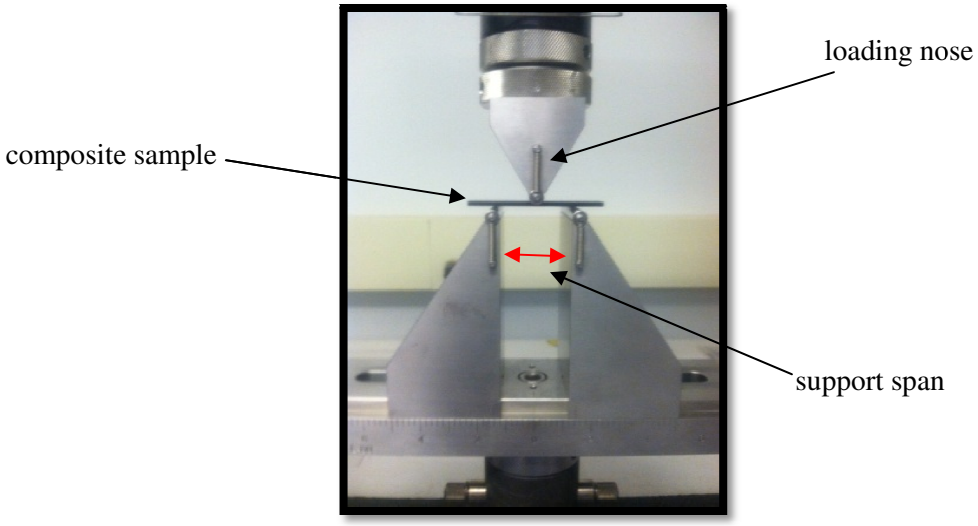

Figure 9: A composite sample resting on the two supports of the Instron 3 point bend test fixture with the loading nose centered between them.

4 point bend testing is similar to 3 point bend testing except that there are two loading noses. The distance between these two loads is known as the loading span and can be seen along with the test fixture in **Figure 10**. The 4 point bend test conducted for this study was executed according to ASTM D 6272-02 [15]. The main difference between the three and four point bend testing is where the maximum bending moment and maximum axial fiber stresses are located. Also, in the 4 point bend test the maximum axial fiber stresses are distributed over the loading span while they are only found directly under the loading nose in 3 point bend testing. The rate of crosshead motion equation for materials that break at comparatively small deflections for this standard is:

$$R = ZL^2/6d \quad (2)$$

This equation resulted in the same crosshead motion rate of 0.038 inches per minute.

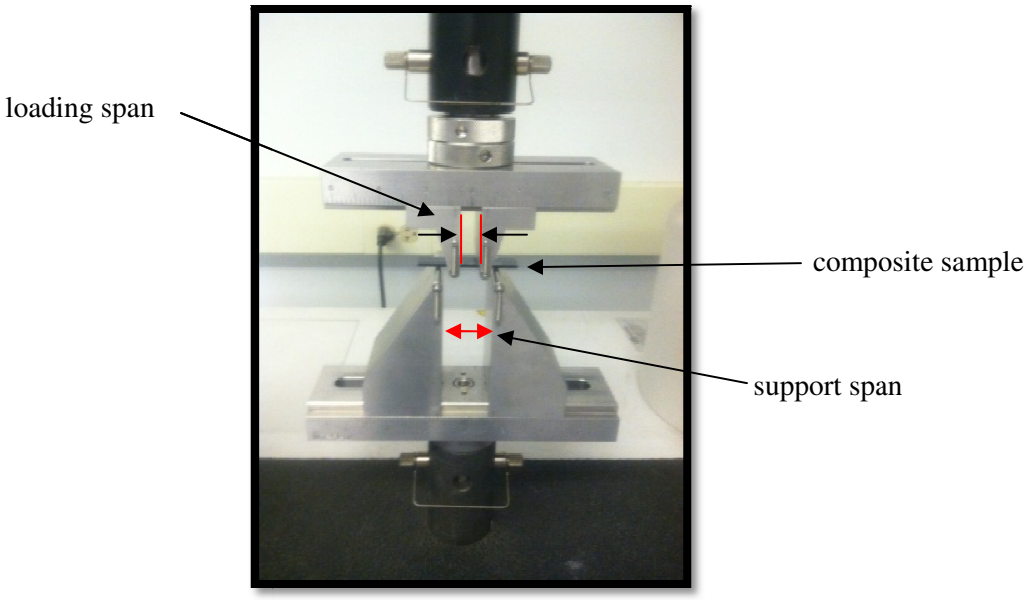

Figure 10: A composite sample resting on two supports with two loading noses.

The flexural test method design and data analysis in this particular project is done through the computer on a program called Bluehill Instron Corporation. After each test is run, Bluehill gives output data as well as showing the fracture load versus extension for each of the samples tested. When loaded in a flexural test set-up, the maximum stress in the outer surface occurs at the midpoint which gives more consistent readings than tensile tests which are more susceptible to cracks. Bluehill will also show the maximum flexural stress that was reached before the specimen broke also known as the flexural strength. These are the values that will be compared with 90 degree tension tensile strength to find correlation between the two tests [(15)].

Comparison and Analysis of Mechanical Testing

The tensile strength values and both types of flexural strength values were then entered into an Excel spreadsheet. With the average tensile strength values on the x-axis and the average 3-point flexural

strength values on the y-axis a straight line was fitted to the data points to find a correlation. Another graph was then made with the same tensile strength values still on the x-axis but the average 4-point flexural strength values on the y-axis. Next, graphs were made for each of the materials using all of the data points to show the range of strength values for each of the materials.

SEM Analysis

After the mechanical testing was complete a sample from each batch was cut so that the fracture surfaces could be imaged with the SEM. The fracture surfaces were cut using a diamond metal wafering blade with a precision saw. The samples were then gold sputtered to avoid charging of the samples and placed on stages to be put in the SEM. The fiber-matrix interactions on the fracture surface of the samples were then examined using the SEM. Images were taken at magnifications up to 3000x for clear imaging of the fibers and matrix. The SEM gave detailed images of the fiber-matrix interface and was useful when comparing materials of similar strength and similar fiber-matrix interactions.

Metallographic Preparation and Analysis

After mechanical and SEM analysis, micrographs were taken to analyze cracks and resin distribution in these composites. In order to see a polished surface of the cross-section for each composite, small samples of each material were mounted in epoxy. The samples were cut using the same diamond saw used for the SEM imaging samples but these samples were taken a good distance away from the fracture surface on the test bars. Epoxy was chosen for mounting because it shrinks less than the other mounting materials and therefore minimizes movement of the sample during curing. The samples were then ground down until the composite was clearly through the epoxy and the polishing began. The samples were polished according to the online ASM Handbook. The samples were ground on wet silicon carbide paper of grits 120, 320, and finally 600 each for 10 minutes. The samples were then given a final polish of 180 seconds on 6 micron, 1 micron, and 0.05 micron polishing wheels [(16)].

Results:

Mechanical Testing Analysis

After the tensile testing was complete, load versus extension graphs were produced by the Bluehill program. These graphs show consistent fracture loads as well as maximum extension for all of the samples of each material (**Figures 11-14**). These graphs give a strong representation of the uniformity or variation between fracture loads as well as the ultimate elongation in each of the four composite sample sets. According to Hooke's law the slope of these lines also represents the stiffness of the material being tested. Too much variation in slope on each of these plots could signify inconsistency in the testing procedure or sample properties. It should also be noted that the first data plot has seven specimen labeled on the graph. The first and second specimen are actually both "sample 1" but had to be run twice because of operator error. The data line labeled "specimen 1" should therefore be ignored and "specimen 2" will refer to sample 1. This exchange can be made because neither of the two lines are outliers.

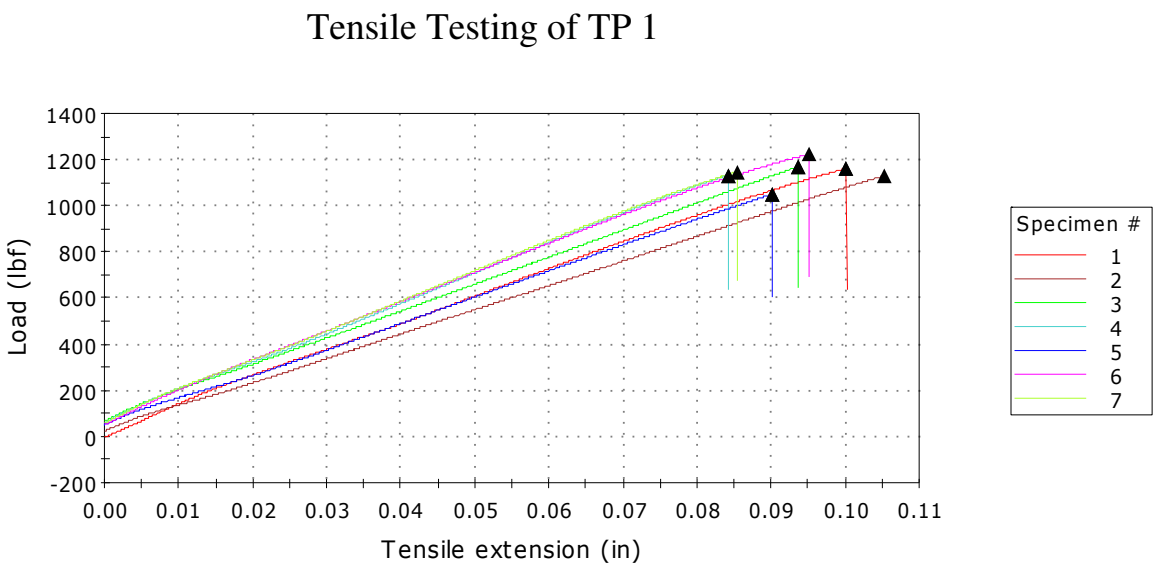

Figure 11: The load versus extension graph for the tensile test data set of TP 1 shows limited variation in stiffness and failure load.

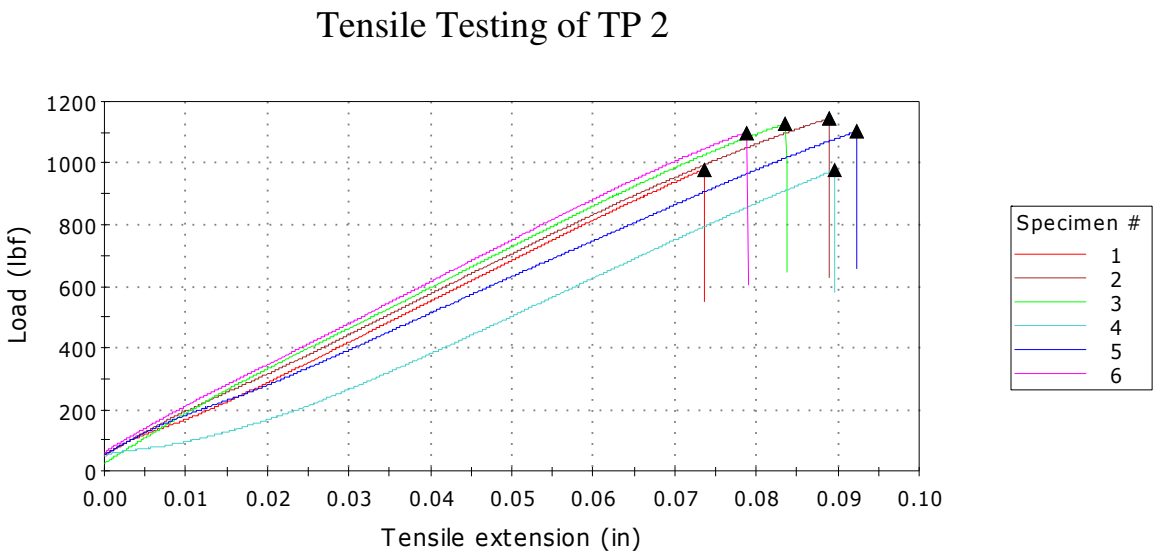

Figure 12: Load versus extension plot for the tensile test data of TP 2 shows a notably lower stiffness for sample 4 and more variation in failure load than was found for the TP 1 data set.

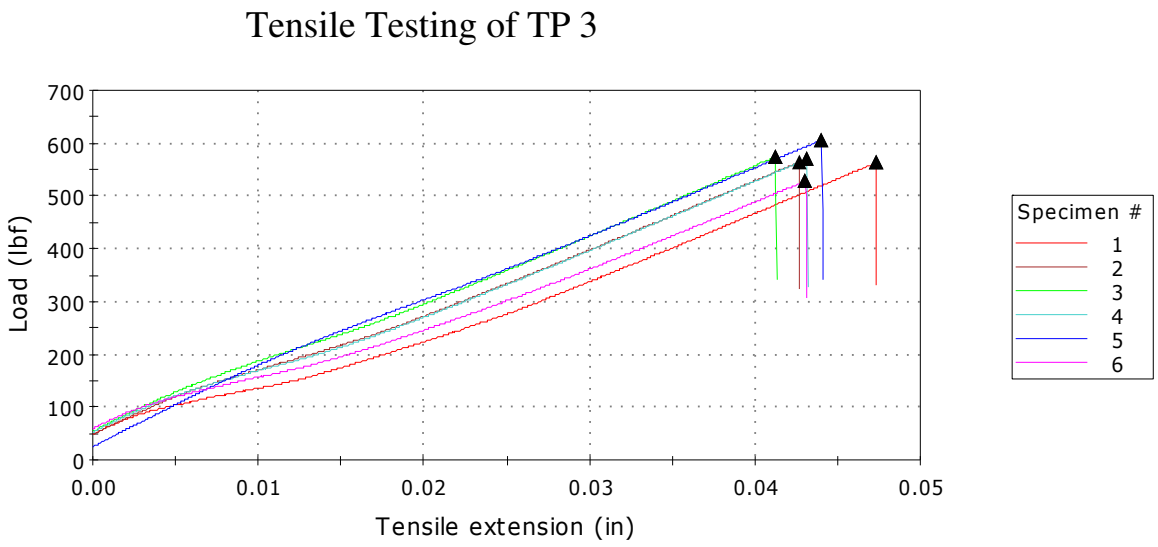

Figure 13: Load versus extension plot for TP 3 shows twice the stiffness shown in TP 1 and 2 and half of the ultimate fracture load.

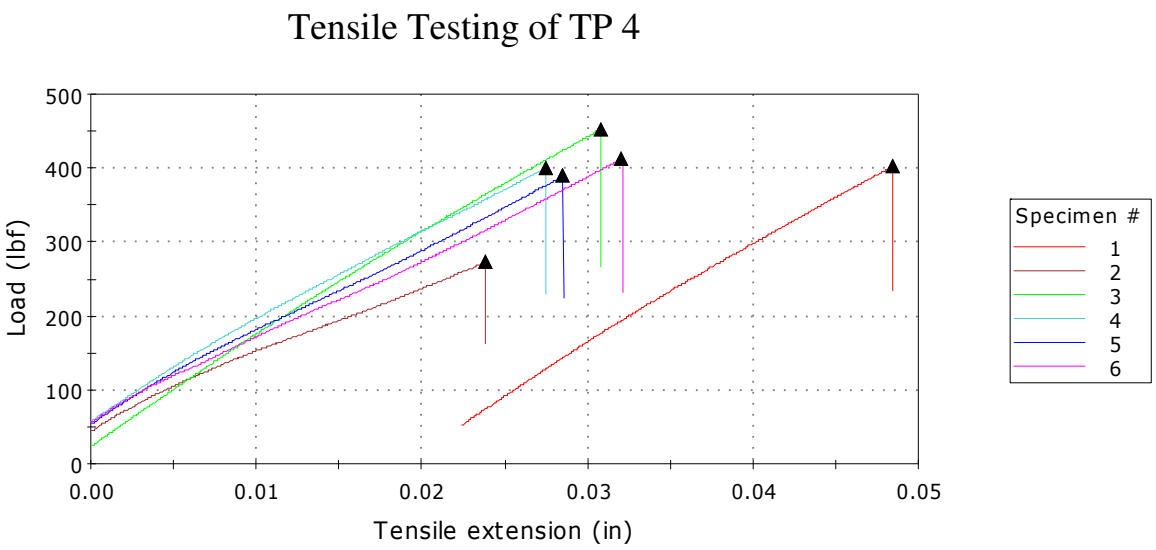

Figure 14: Load versus extension plot for TP 4 shows higher stiffness than any of the other materials as well as an outlier.

The 3 and 4 point bend test data was then graphed on flexural load versus extension plots. These test results show almost no variation in stress for each material data set. Because of the low fracture loads of these test methods the range of flexural loads happens on a much smaller scale but still should not be ignored (**Figures 15-22**).

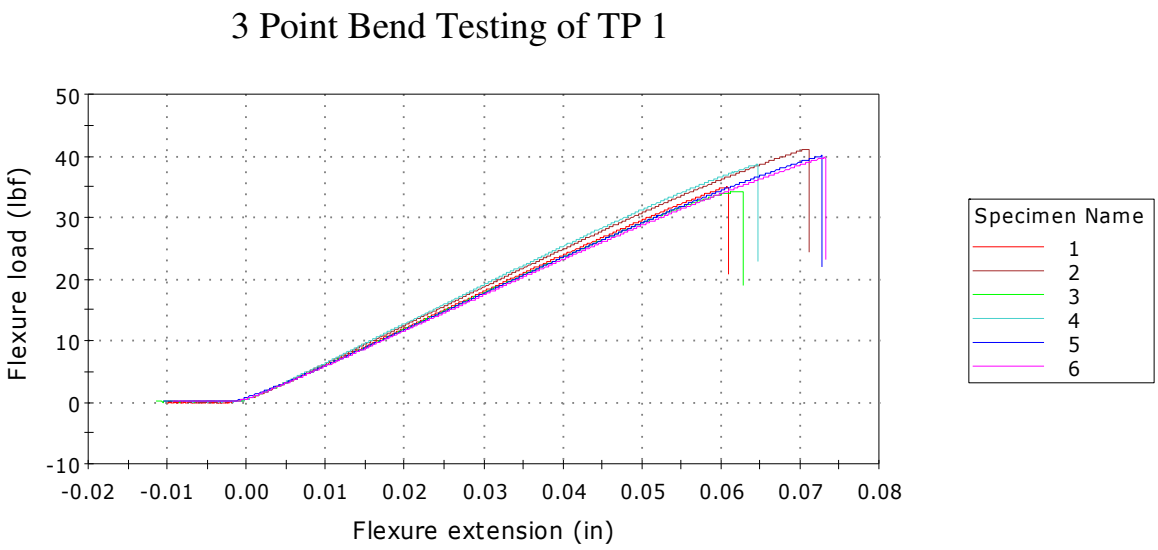

Figure 15: Flexural load versus extension plot for the 3 point bend test data on TP 1 shows minimal variation on any of the properties displayed.

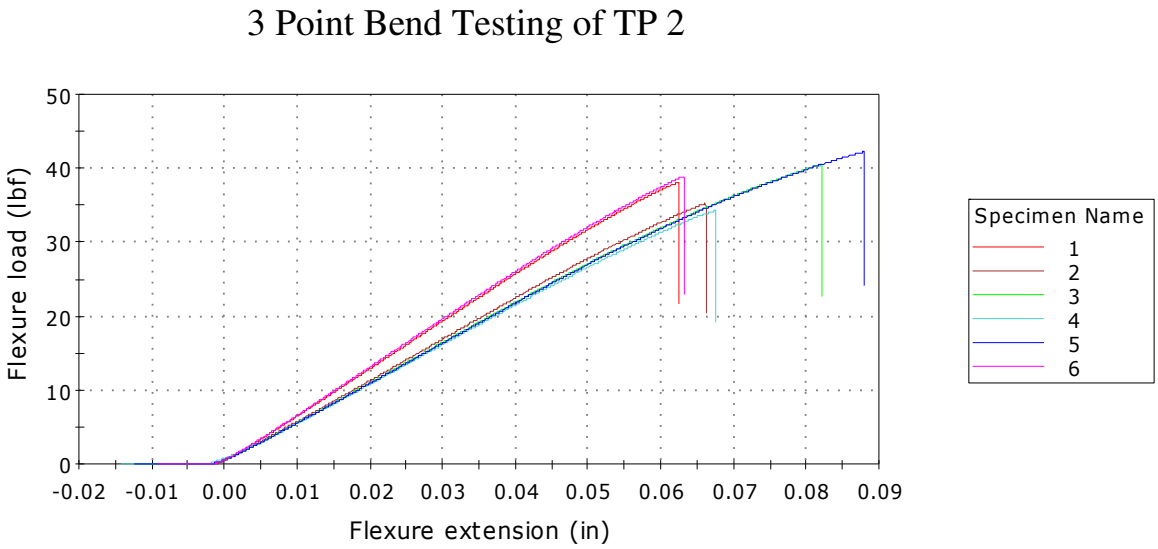

Figure 16: Flexural load versus extension plot for the 3 point bend test data on TP 2 shows a higher range of ultimate flexural extensions as well as stiffness values.

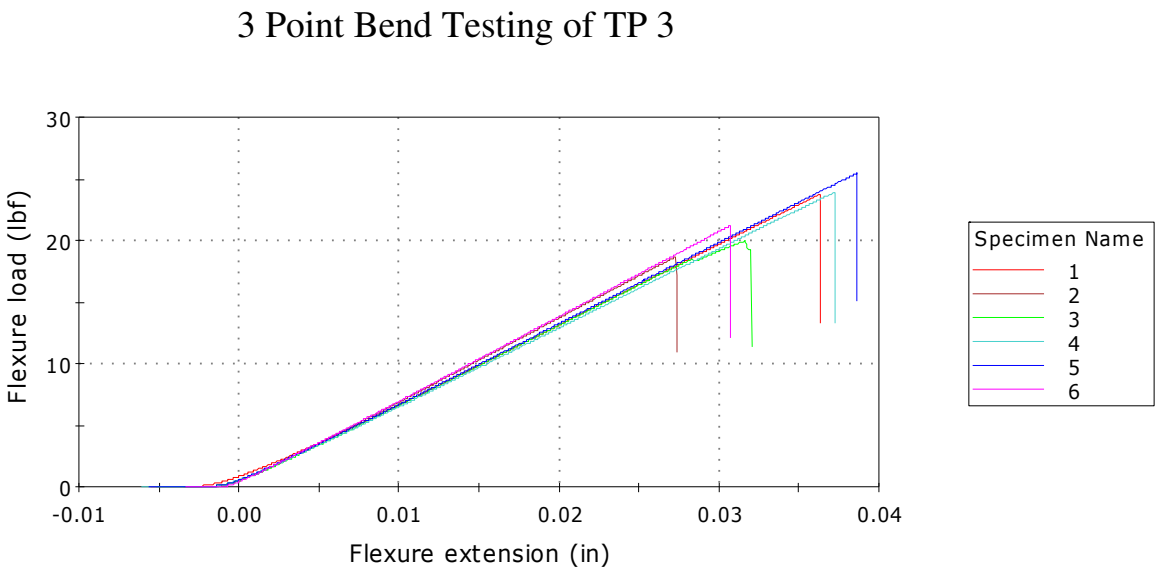

Figure 17: This flexural load versus extension plot for the 3 point bend test data of TP 3 shows all of the ultimate flexural loads to be under 30 lbf.

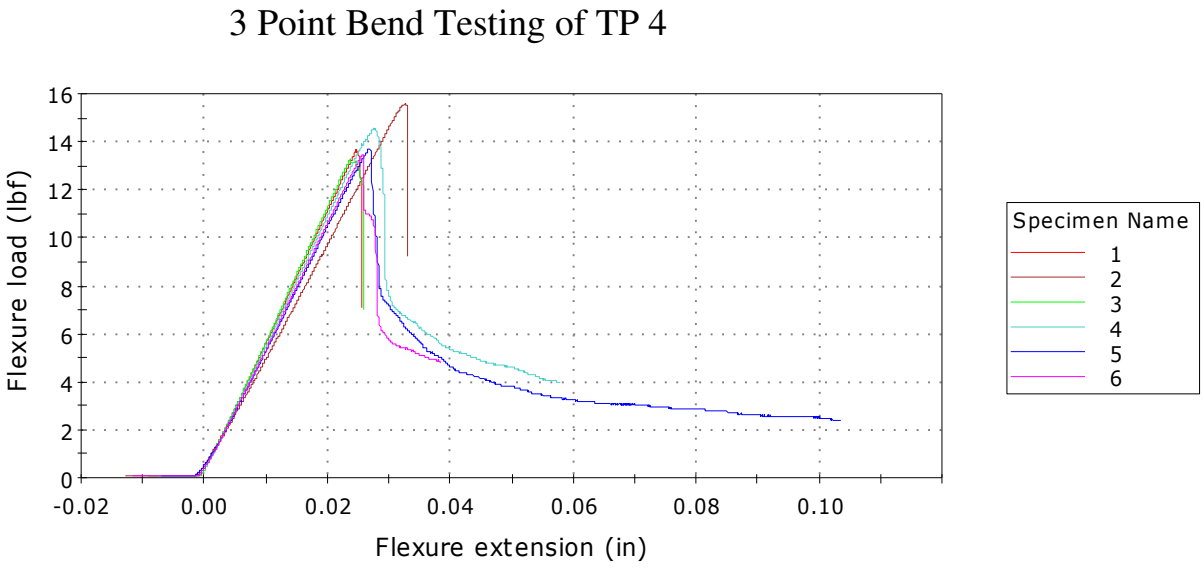

Figure 18: The flexural load versus extension plot for TP 4 shows all of the ultimate loads to be under 16 lbf and relatively high stiffness.

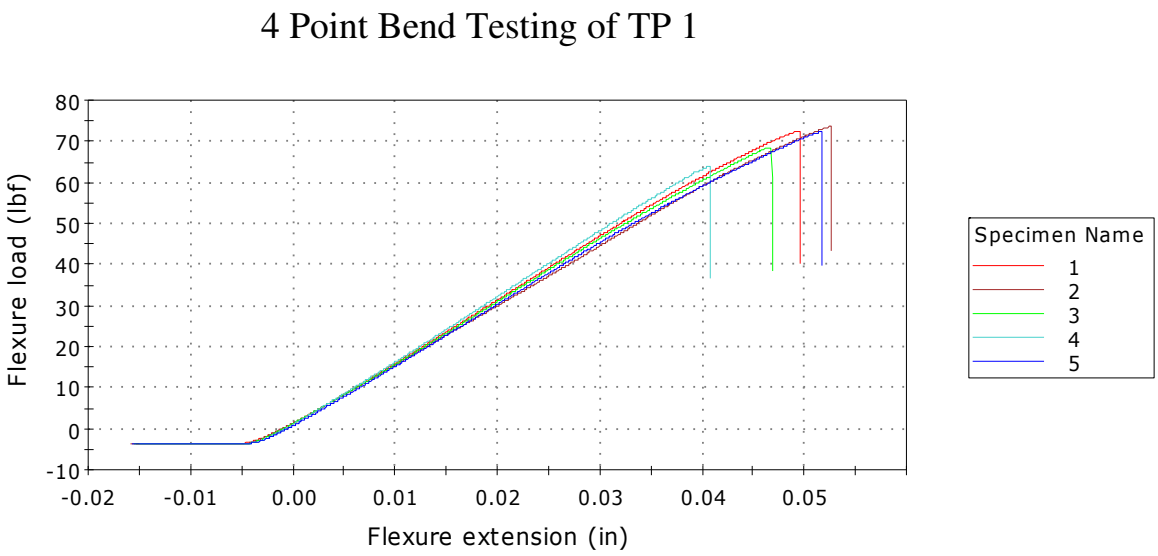

Figure 19: This flexural load versus extension plot shows little to no variation in the stiffness of the samples as well as consistent ultimate flexural extensions and ultimate flexure loads.

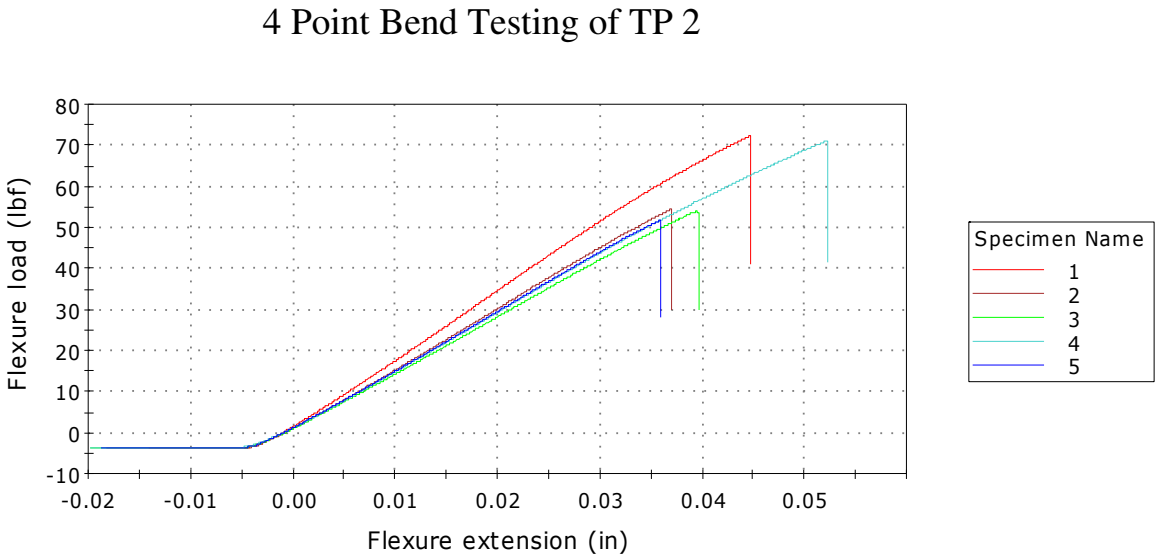

Figure 20: This flexural load versus extension graph shows significant data scatter with load as well as variance in stiffness for the first sample.

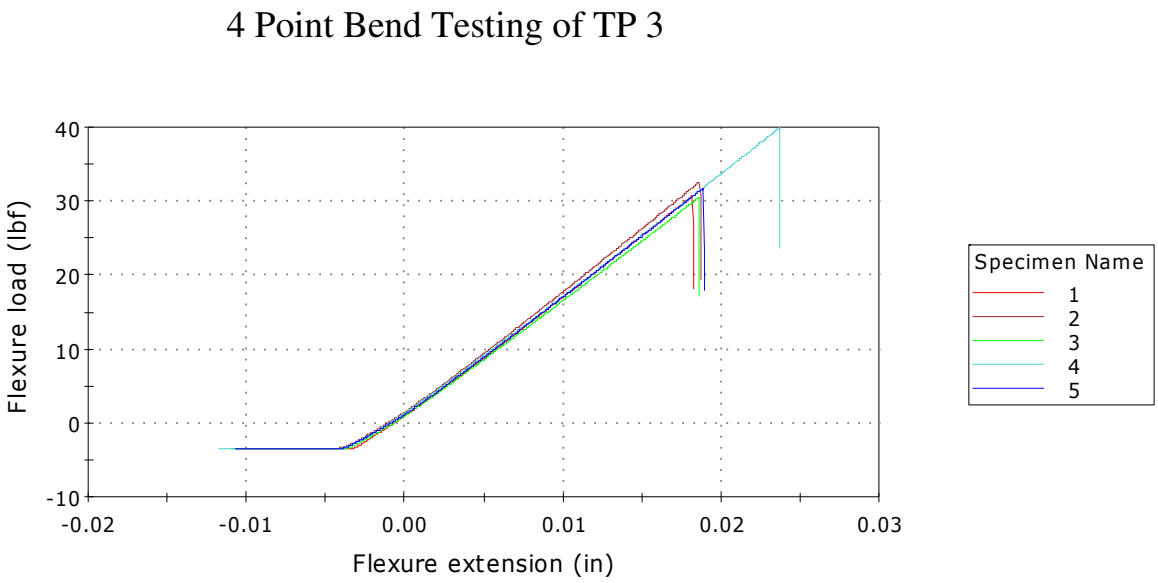

Figure 21: This flexural load versus extension plot shows a definite outlier in ultimate flexural load in an otherwise uniform data set.

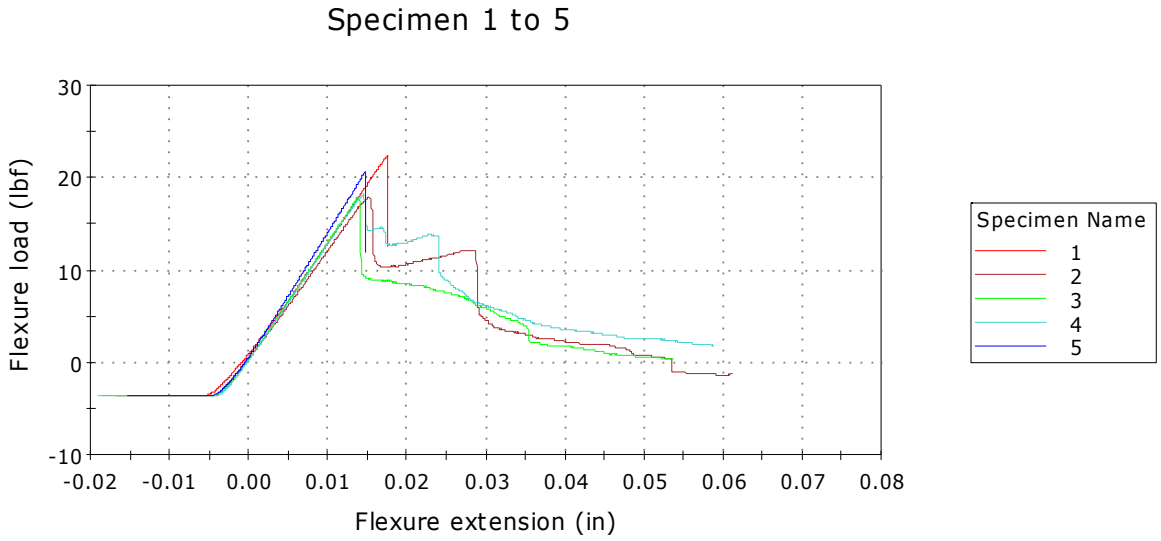

Figure 22: The flexural load versus extension plot of TP 4 shows high stiffness and low strength. The continuation of the plot after the ultimate load is due to the sample not fracturing completely at failure.

After these plots were generated and analyzed, the data was converted into tensile strength and flexural strength values. The standard deviation of these data sets never exceeded 2.67 ksi and so it was

considered sufficient to average the data sets and compare those values. In the initial review of the data there was an obvious progression of maximum strength in the materials with TP 1 having the highest and TP 4 having the lowest. There was also a significant gap between the maximum strength values of the first two materials and the second two. TP 1 and TP 2 had such similar strengths that their strength values overlapped. This caused the mean of TP 2 to actually be higher in magnitude than that of TP 1 (**Table III**).

Table III: Mean strength values of each of the 4 materials found from each of the three tests

Material	Tensile Strength (ksi)	3 Point Flexural Strength (ksi)	4 Point Flexural Strength (ksi)
TP 1	13.03	20.42	18.34
TP 2	12.43	21.14	16.8
TP 3	6.01	10.65	7.99
TP 4	4.35	7.55	5.35

The flexural stresses from the bend test data were then graphed versus the tensile strengths to find a correlation between the two tests. The first graphs made used all of the data points and were separated by material. These graphs did not show the strong correlation that was intended and were difficult to interpret with such few data points (**Figures 23-26**). These graphs do however show a representation of the range of stress values for each material. This helps to get an idea of how consistent the readings were for each material and how reliable the data is.

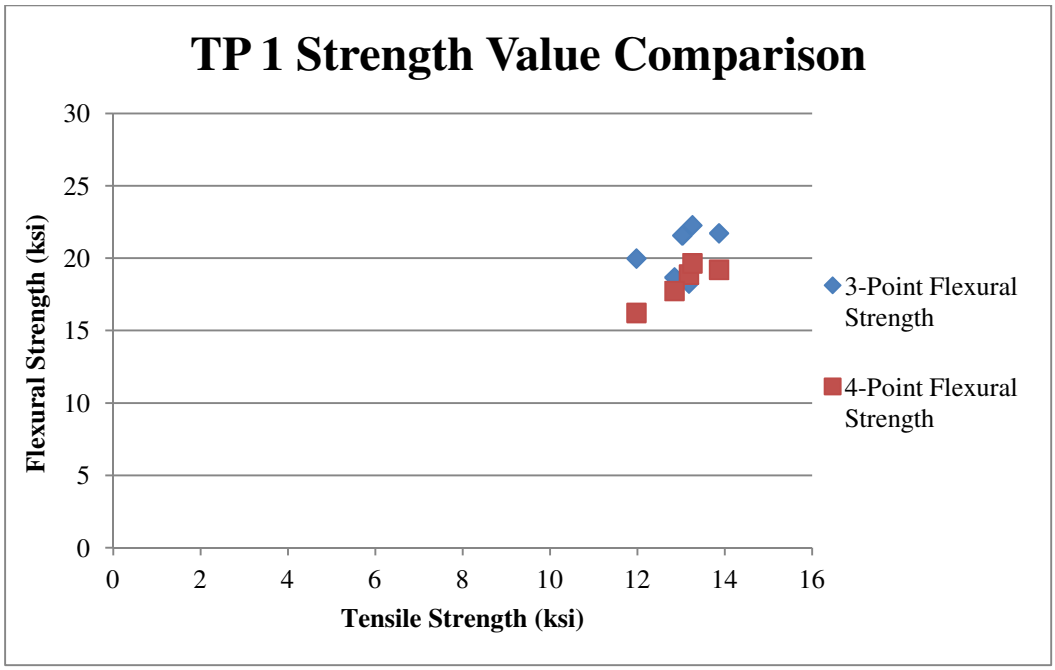

Figure 23: There is minimal variation in the flexural and tensile strength values plotted against each other for TP 1.

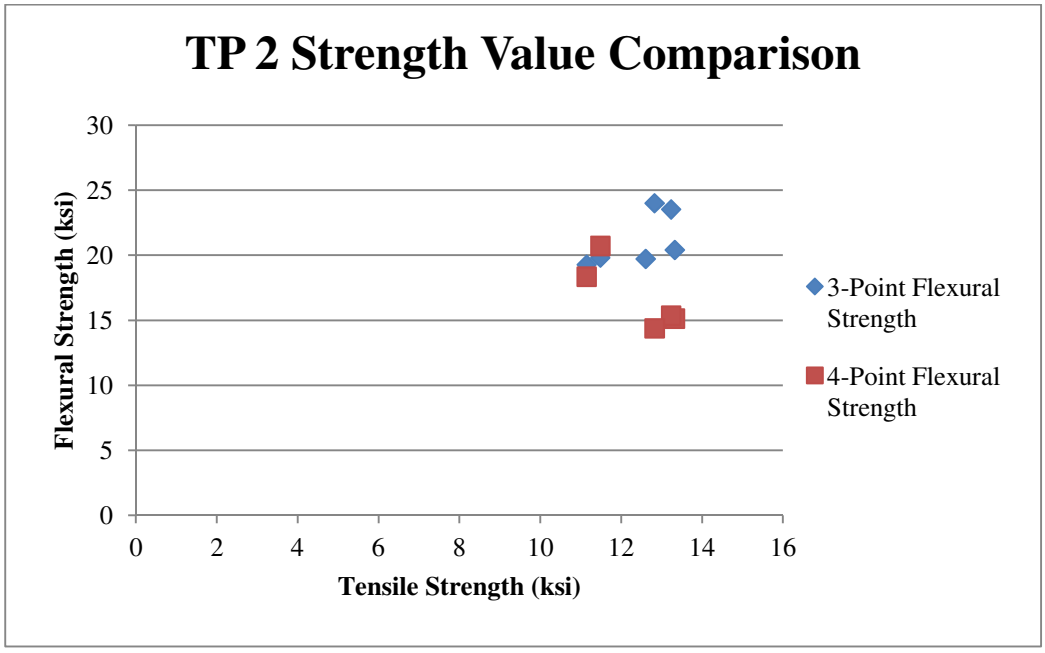

Figure 24: There is a wider range than TP 1 of both flexural and tensile strength values for TP 2.

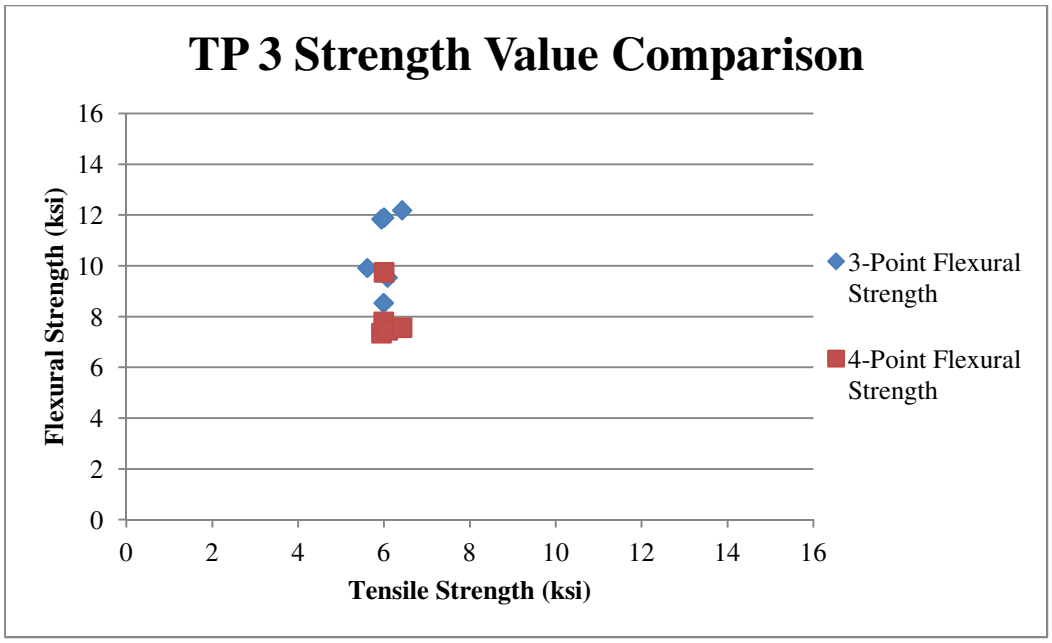

Figure 25: This graph illustrates a narrow range of tensile strength values with a wider range of flexural strength values than TP 4.

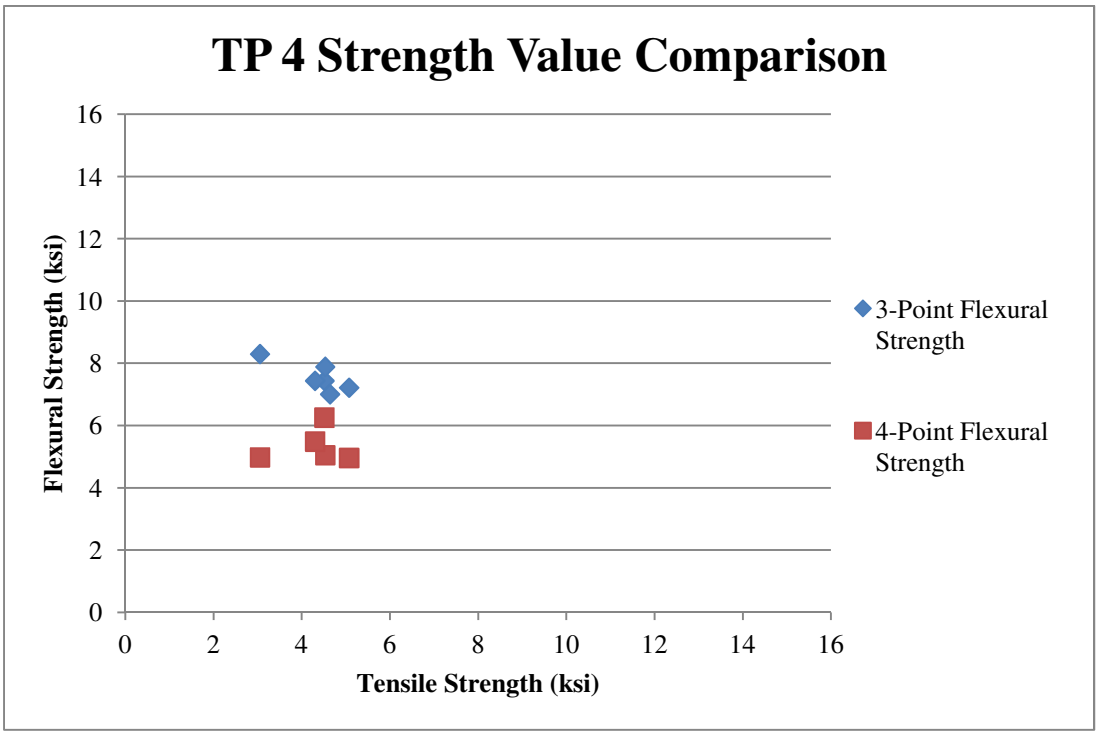

Figure 26: This graph shows a wider range of tensile strength than TP 3 with a smaller range of flexural strength values.

The next two graphs made showed the average flexural and tensile stress for all four materials with separate graphs for 3 and 4 point values. The graphs were made in excel and a straight line was fitted to them with an R^2 values given to quantify the correlation (**Figures 27-28**). These graphs show that as the tensile strength increases, the flexural strength also increases. Although the values are not necessarily the same, the trend from weakest to strongest material is the same.

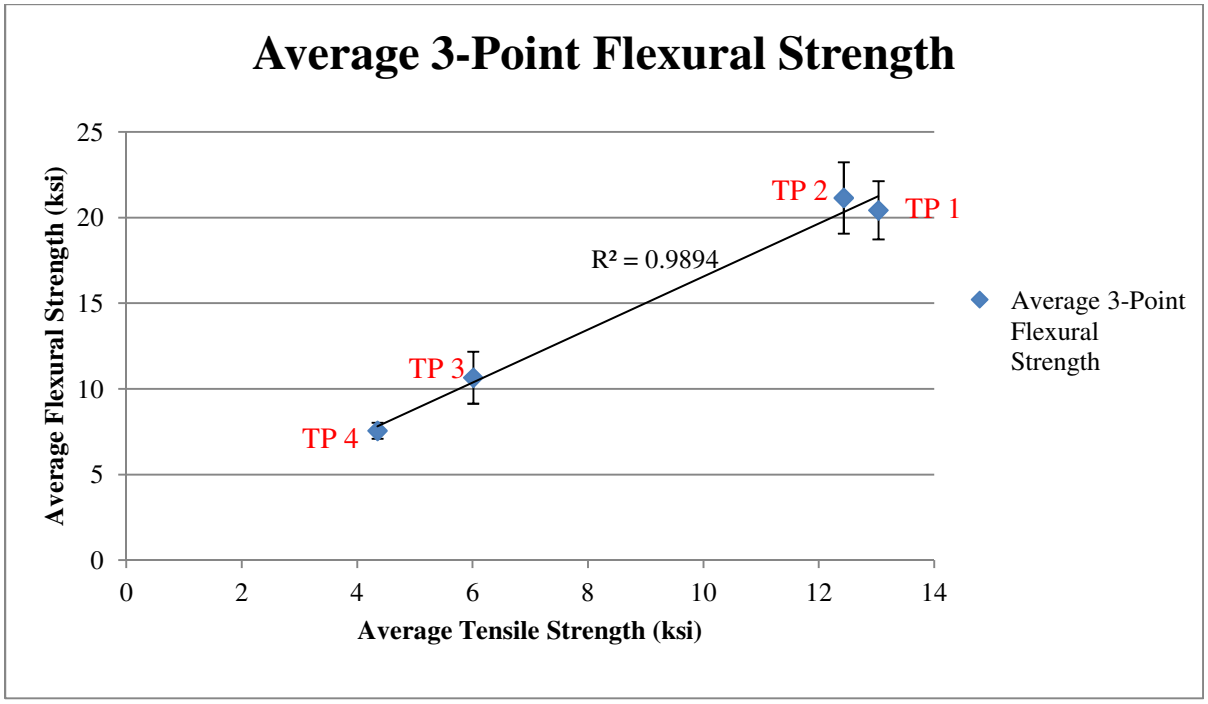

Figure 27: This graph demonstrates the strong correlation between the average 3 point flexural strengths and average tensile strengths for all four materials.

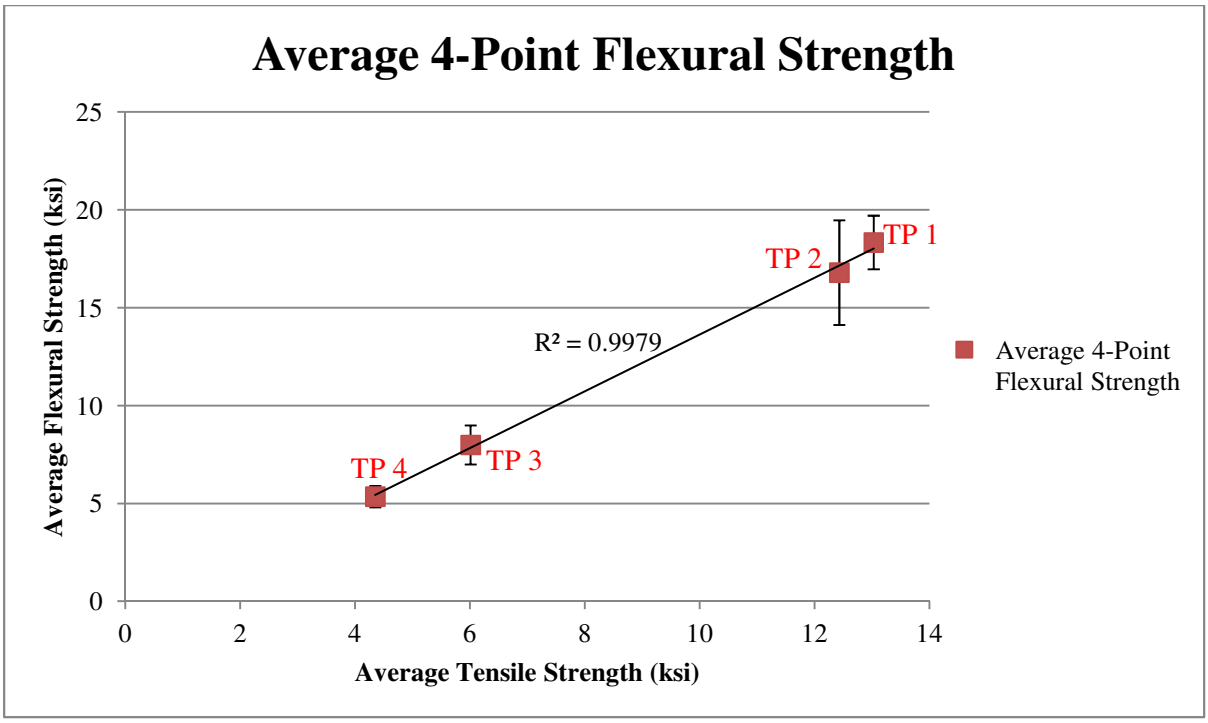

Figure 28: This graph demonstrates the strong correlation between the average 4 point flexural strength and the average tensile strength for all four materials.

The R^2 values came out to be 0.9894 for 3 point bend data points and 0.9979 for 4 point bend data points which means there is a strong correlation between tensile stress and flexural stress.

SEM Analysis

As predicted, the SEM images taken showed that as the fiber-matrix bond strength increased, the strength of the composite increased as well (**Figures 29-35**). The microstructure of each of the varying resins impacted their ability to wet the fibers and then adhere to them. The following images show the increase in fiber-matrix adhesion from the weakest material to the strongest. During imaging there was no visible difference in the fiber-matrix interaction between the three different test mechanisms. Because of this, there is not necessarily an image of each of the three test fracture surfaces for each of the

materials. Rather, the most focused and relevant images were chosen and used in this report. As the images progress, an increased amount of resin still adhered to the fiber can be observed.

In the images of TP 4, there is a clear separation between the fiber and matrix because of the weak bond between the two. The thermoplastic matrix found in this composite did not properly wet the fiber and therefore did not adhere well. Moving to the images of TP 3 there is a slight increase in resin left on the fibers post-fracture. This increase reveals an increase in strength of the bond between the fiber and matrix. The images of TP 2 show the fiber-matrix bond unbroken even after the fracture of the material. These images demonstrate fracture that relates to the toughness of the matrix rather than the weak bonds between matrix and fiber. Similar trends are shown in the images of TP 1 which gives further proof of the similarities between those two composites.

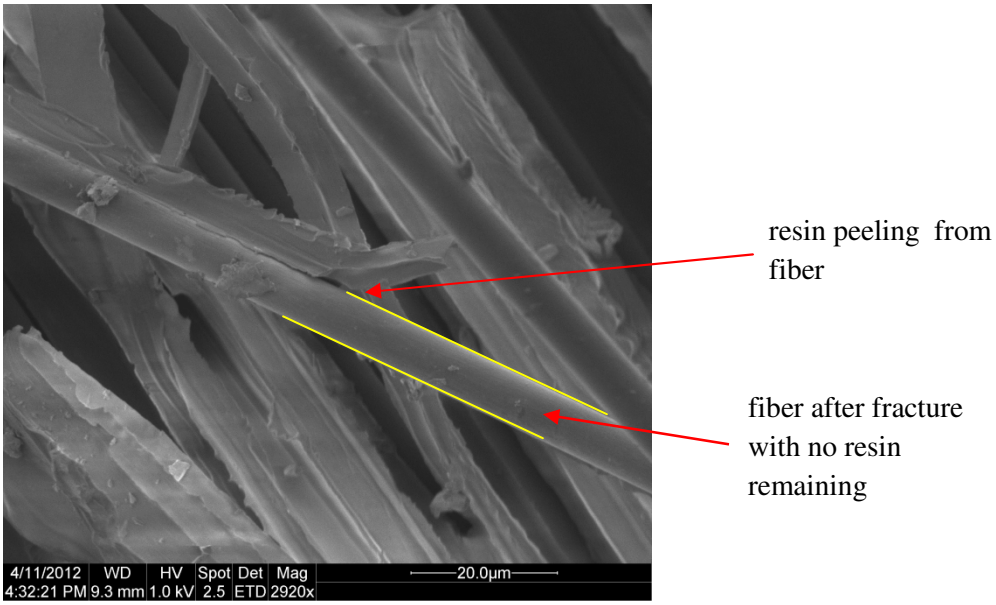

Figure 29: Clean break between fiber and matrix on the fracture surface of TP 4 after 3 point tensile testing.

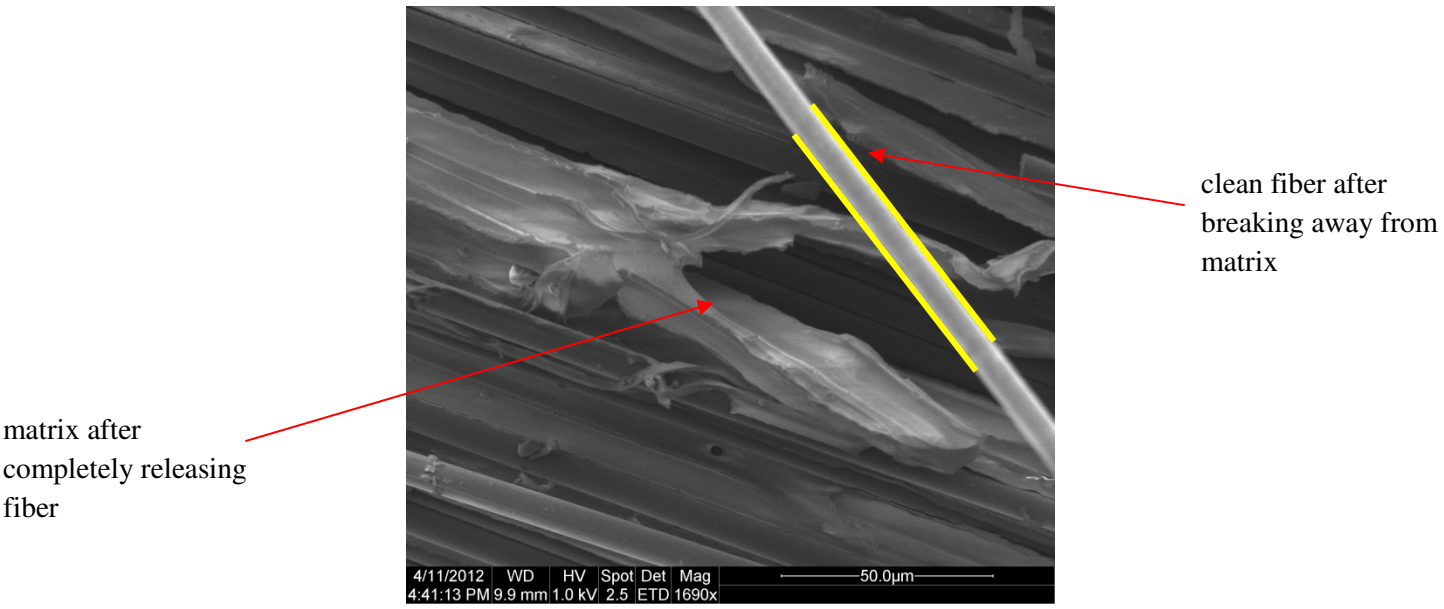

Figure 30: The complete release of fiber from the matrix on the fracture surface of TP 4 after 4 point bend testing showing poor adhesion between fiber and matrix.

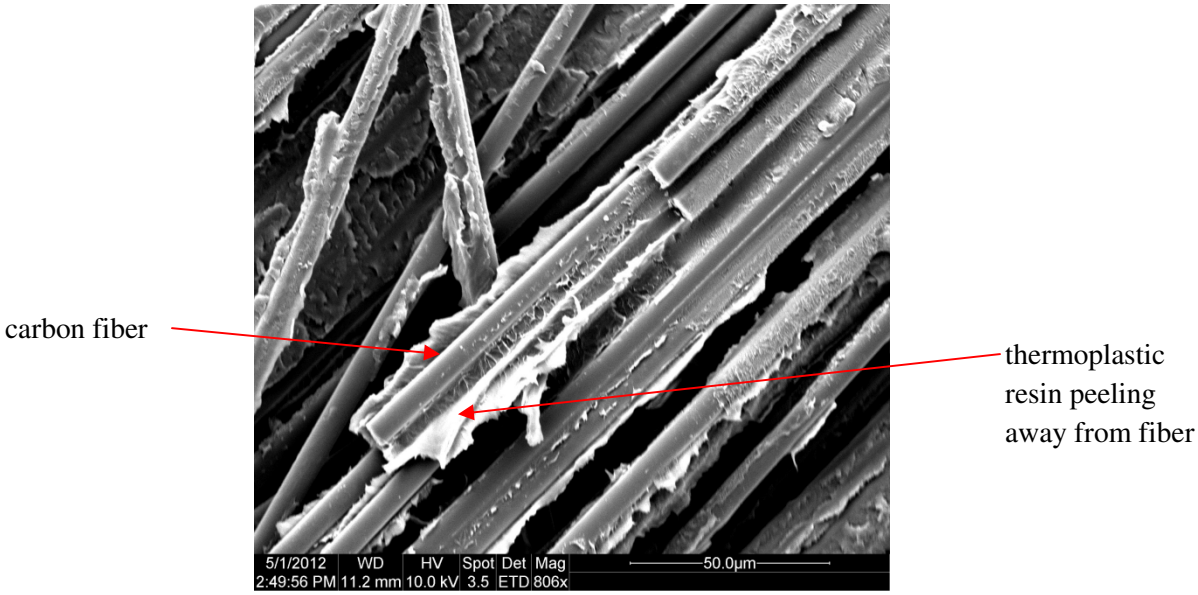

Figure 31: The unraveling of matrix around the fiber on the fracture surface of TP 3 after 4 point bend testing.

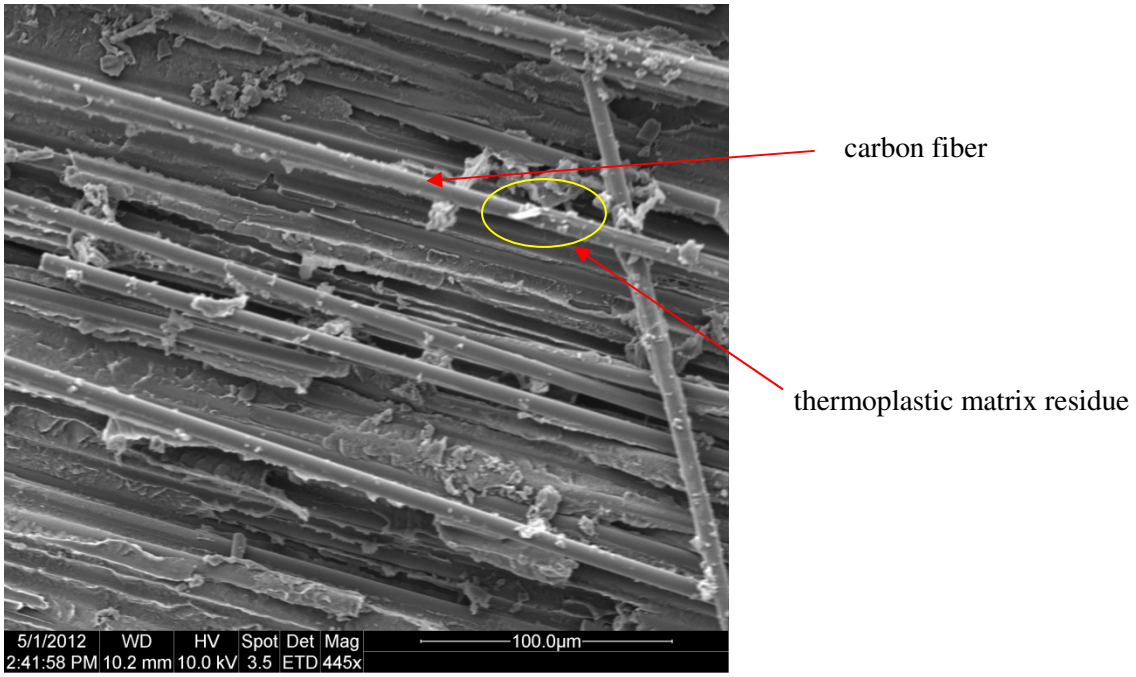

Figure 32: Minimal residue of matrix on the fibers of TP 3 after fracture by 3 point bend testing shows weak bond between fiber and matrix.

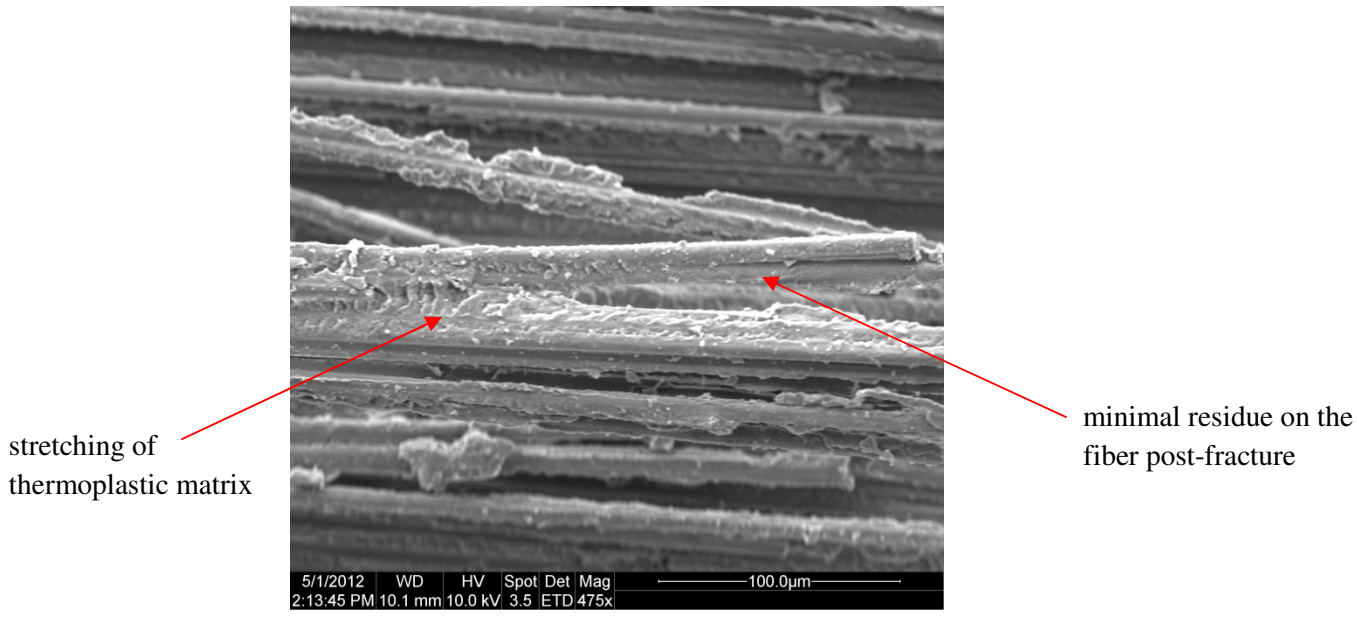

Figure 33: Resin stretching to maintain grip on the fiber on the fracture surface of TP 3 after tensile testing.

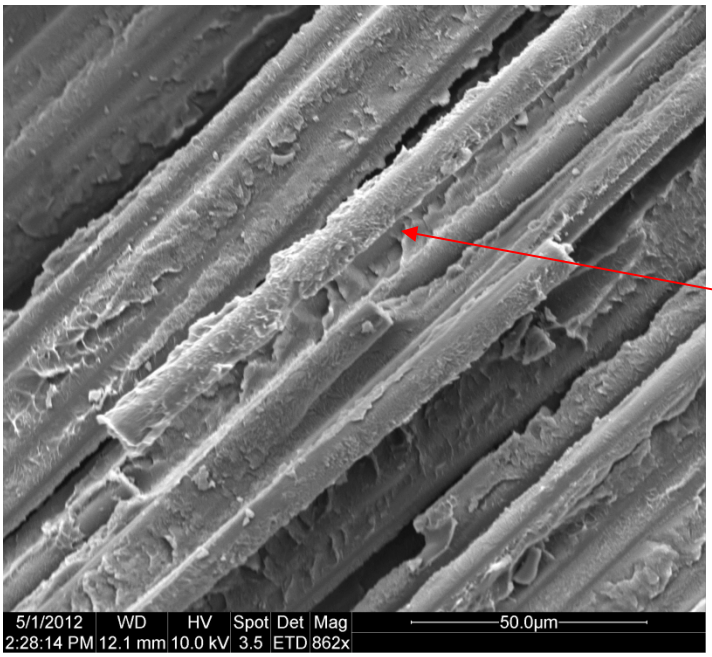

Figure 23: Significant amount of matrix still bonded to the fiber after the fracture of TP 2 by 4 point bend testing.

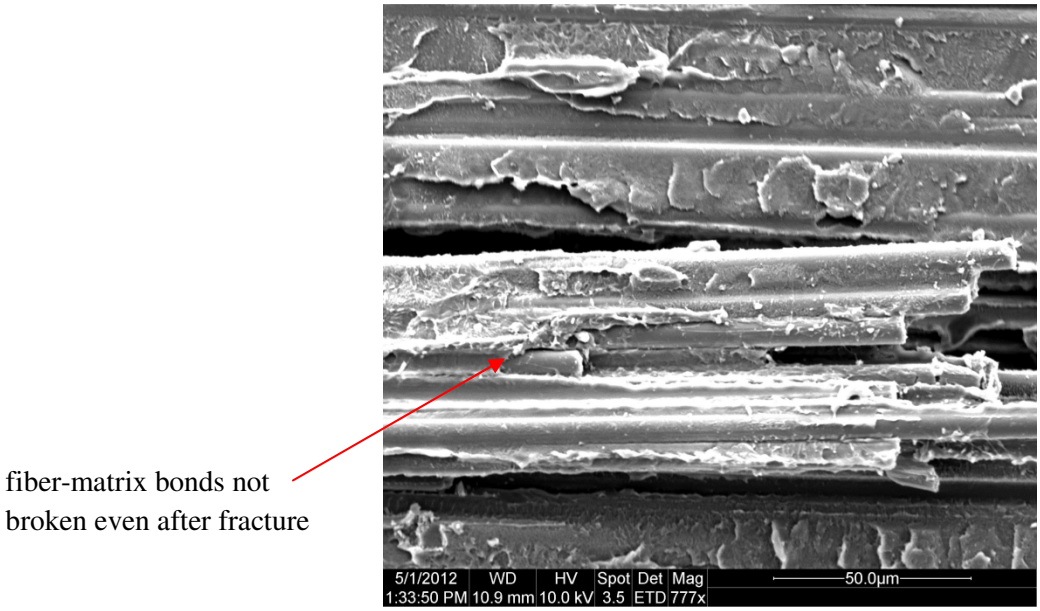

Figure 34: Limited separation of fiber and matrix, even after fracture of TP 1 by tensile testing.

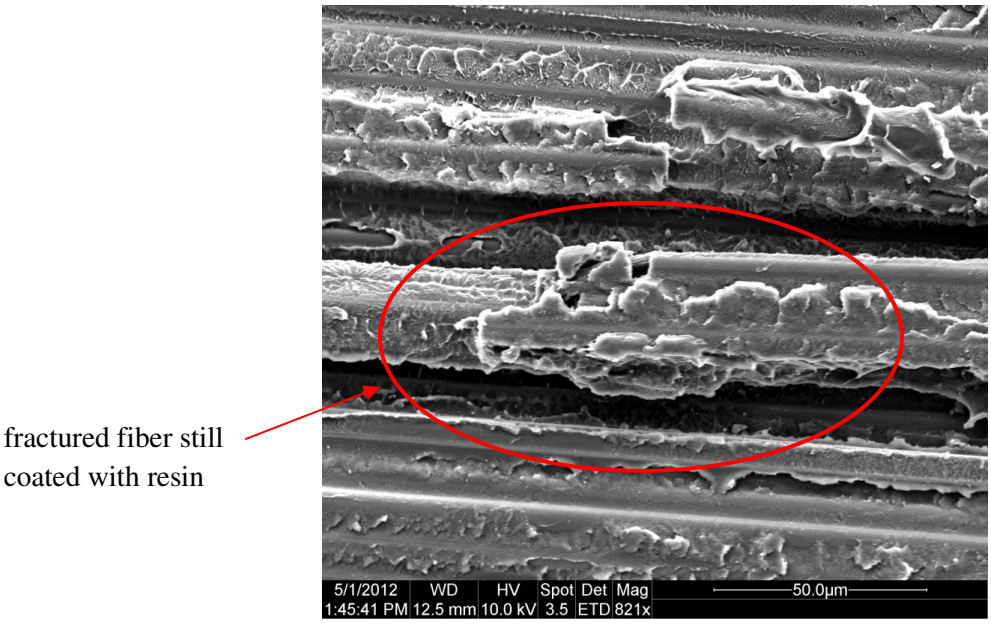

Figure 35: Attachment of fiber and matrix even after failure on fracture surface of TP 1 after 3 point bend testing.

Metallographic Imaging and Analysis

At the end of each polishing cycle the samples still seemed to have some residue stuck within the microstructure and so the samples had to be sent to TenCate for further polishing. When the samples returned from TenCate they were imaged at 200x and 500x magnifications **(Figures 36-43)**. The images taken at 200x give visual representation of the resin distribution within the composites. The images taken at 500x are used to give a closer look at the fiber-matrix interface and to check for any voids or cracks.

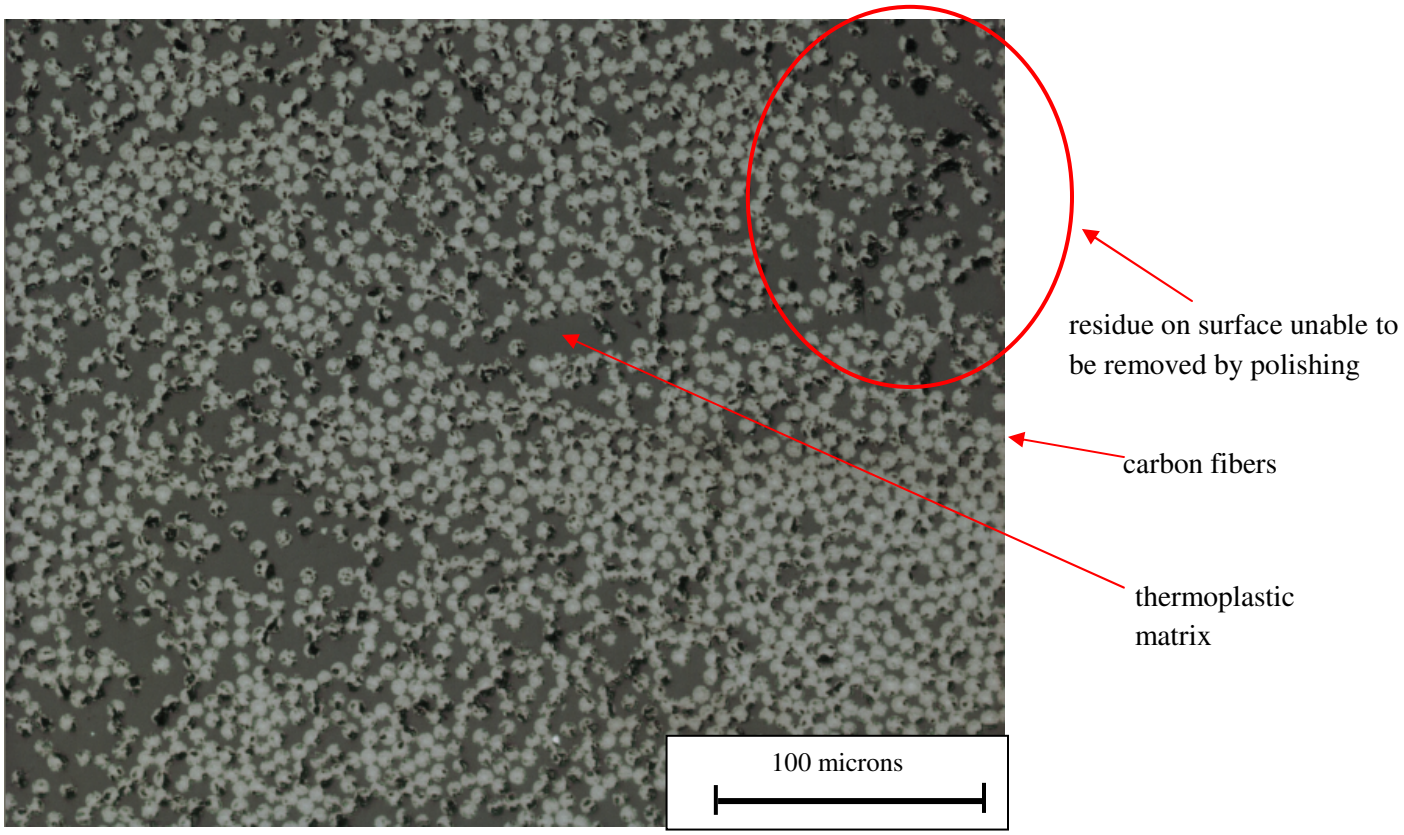

Figure 36: 200x micrograph of the cross-section of TP 1 shows even resin distribution as well as residue remaining after polishing.

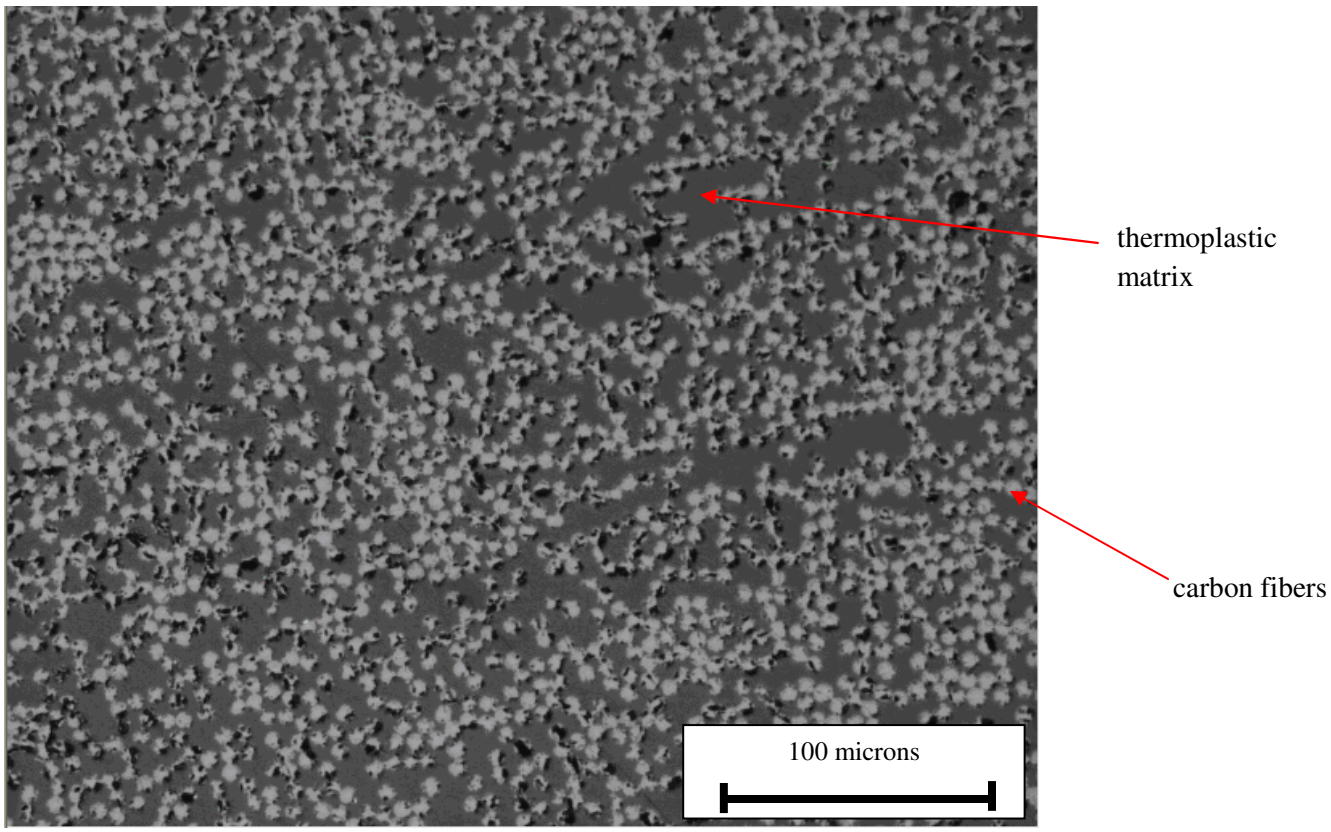

Figure 37: 200x micrograph of cross-section of TP 2 shows even resin distribution.

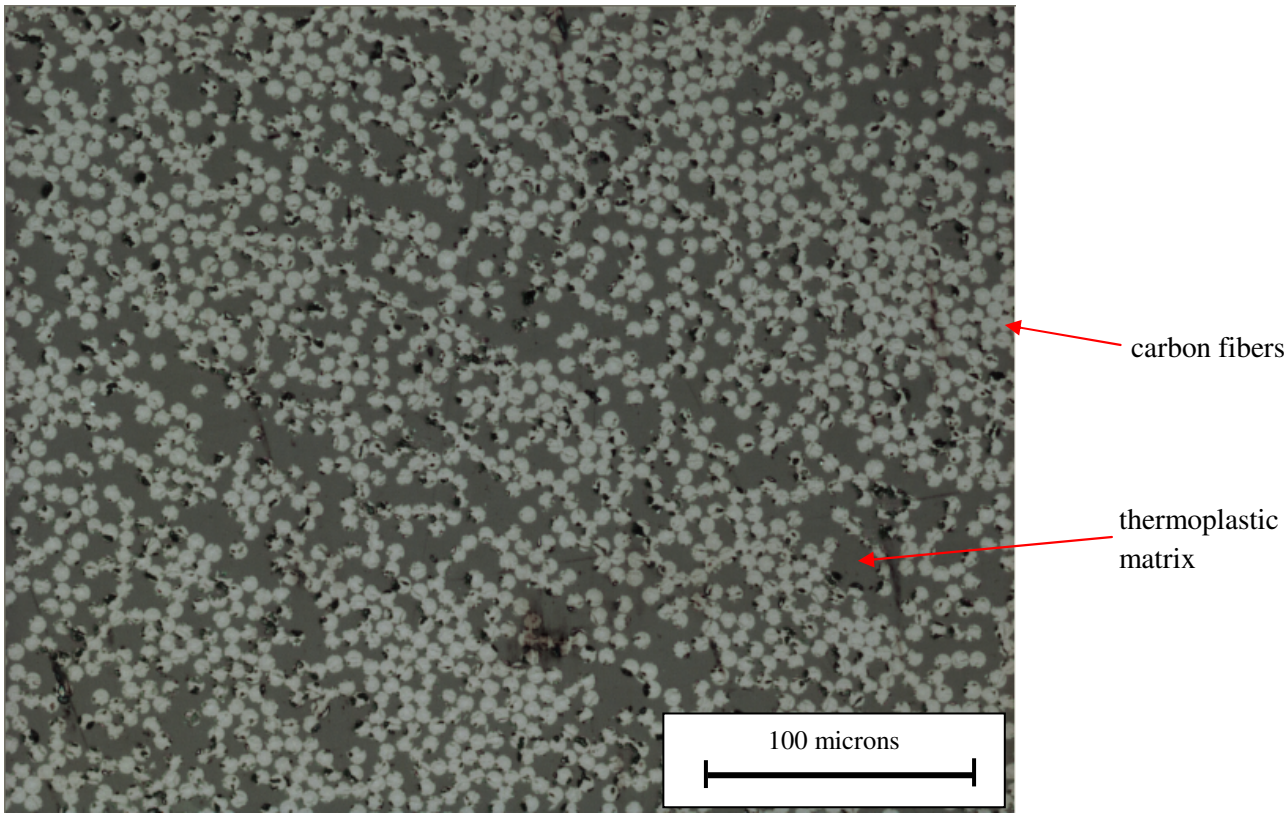

Figure 38: 200x micrograph of cross-section of TP 3 shows less residue after polishing than TP 1 and 2.

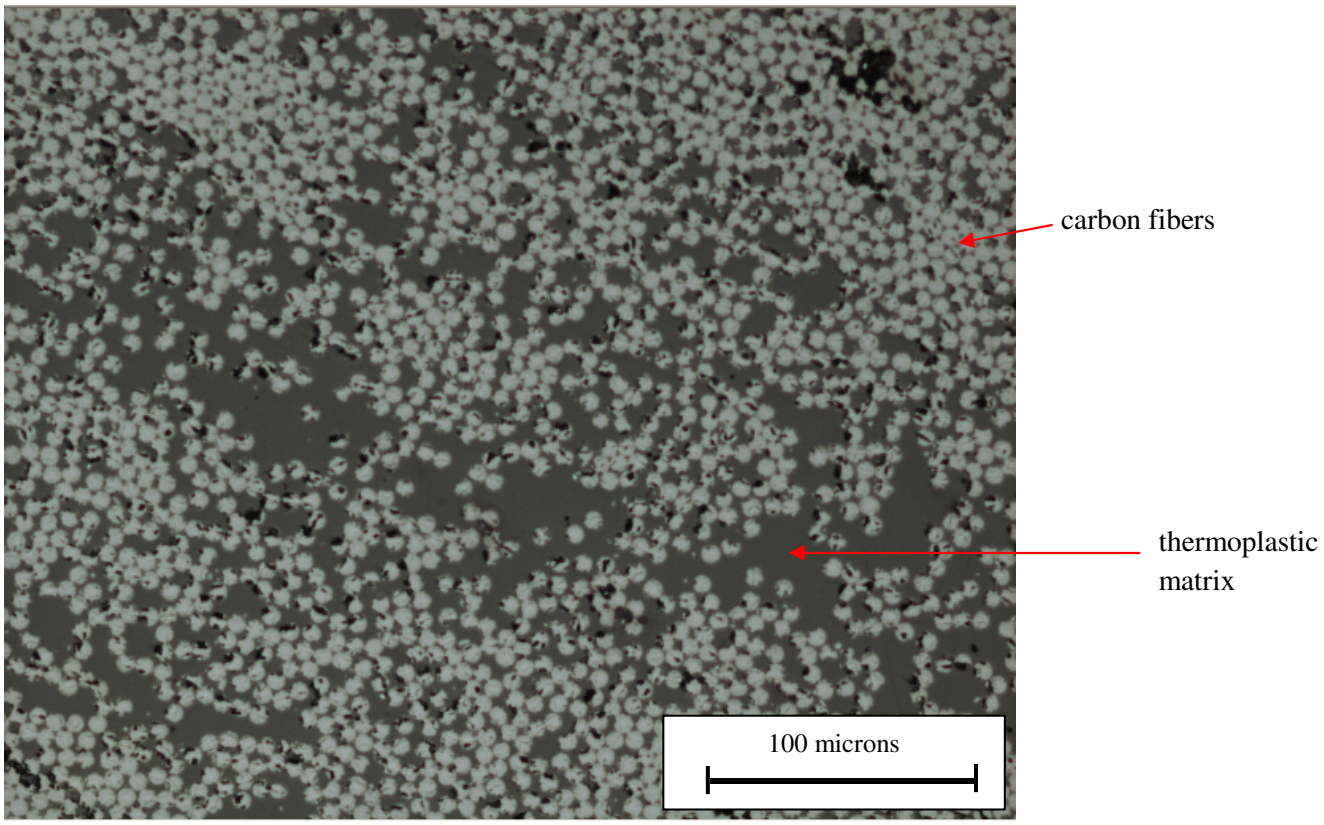

Figure 39: 200x micrograph of cross-section of TP 4 shows sections of uneven resin distribution.

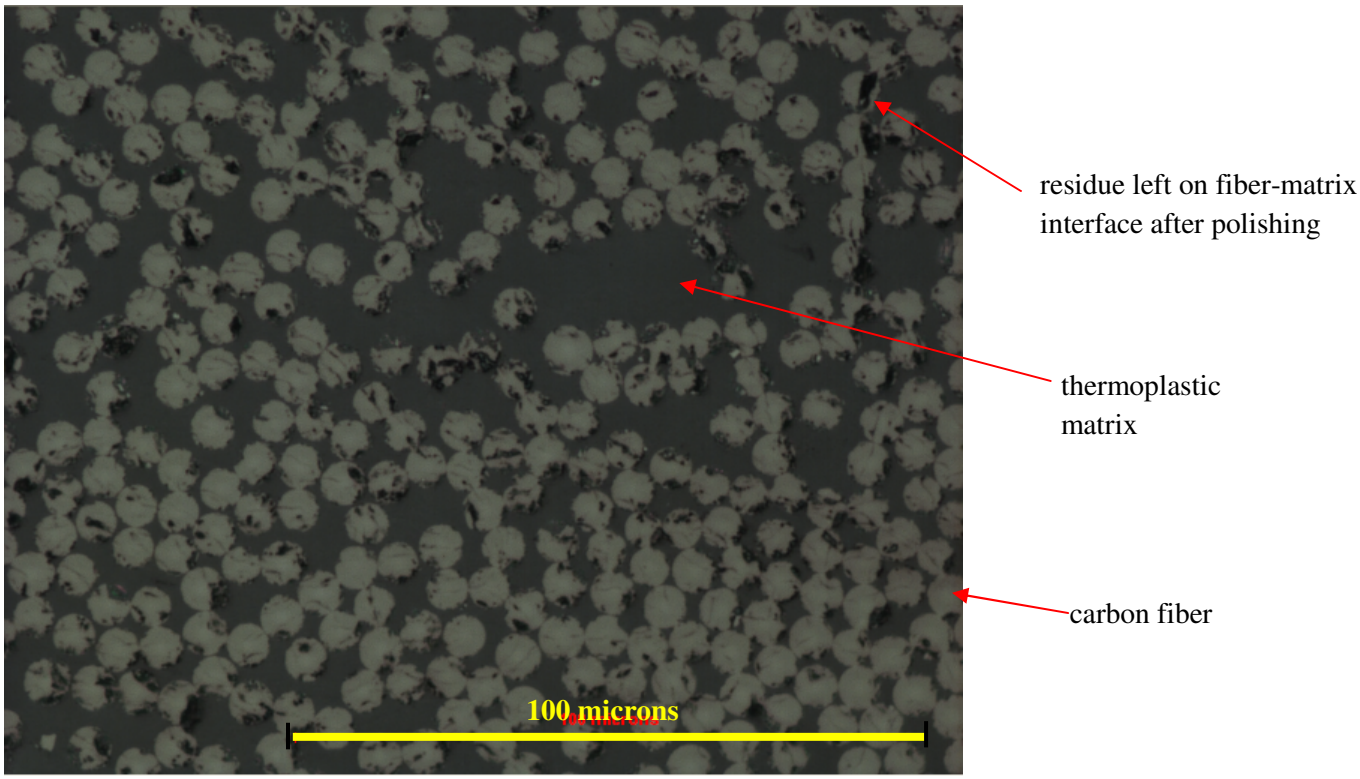

Figure 40: 500x micrograph of TP 1 shows minimal residue left after polishing.

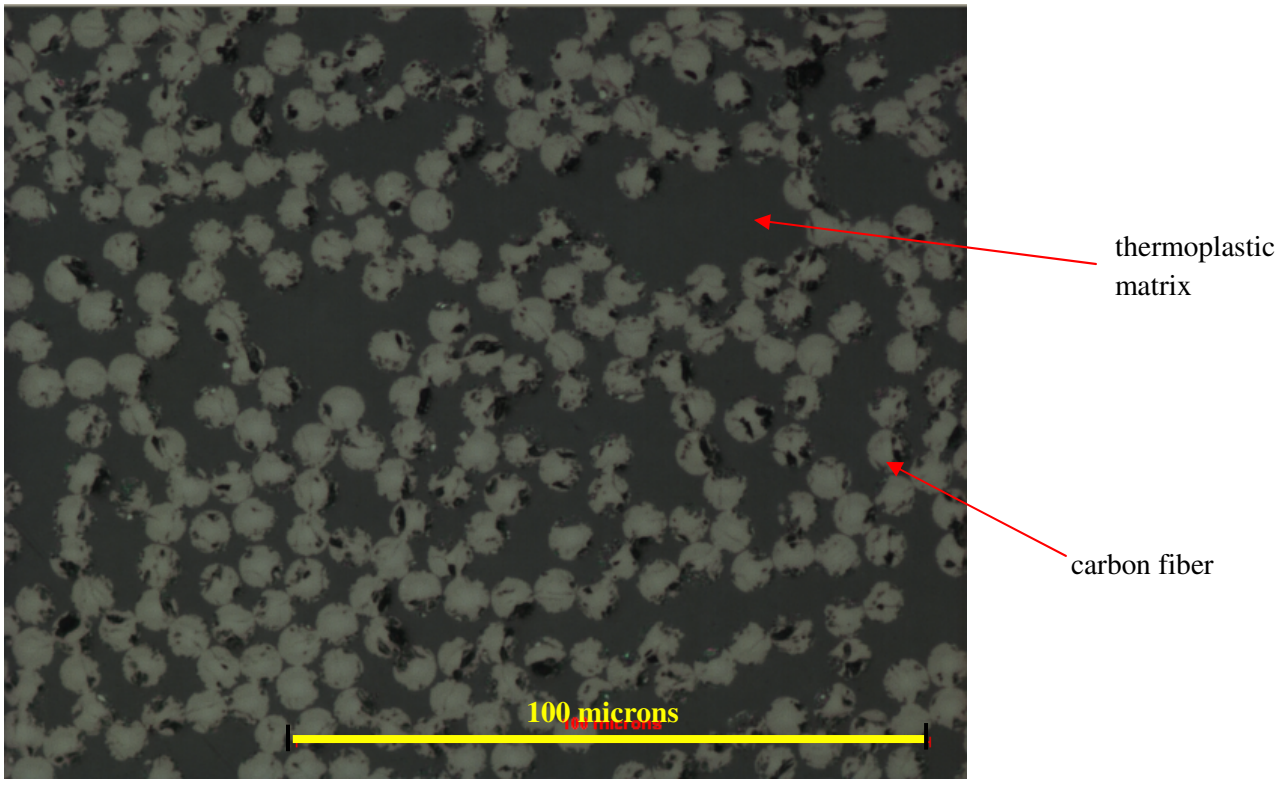

Figure 41: 500x micrograph of TP 2 cross-section shows minimal residue after polishing.

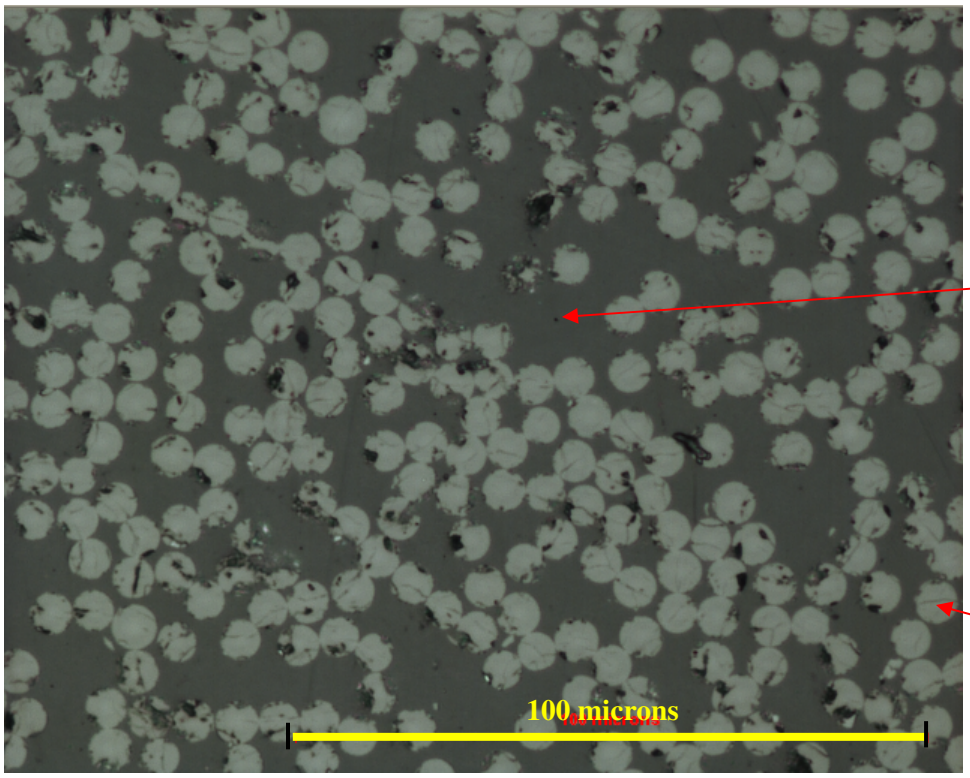

Figure 42: 500x micrograph of cross-section of TP 3 shoes less even resin distribution than TP 1 and 2.

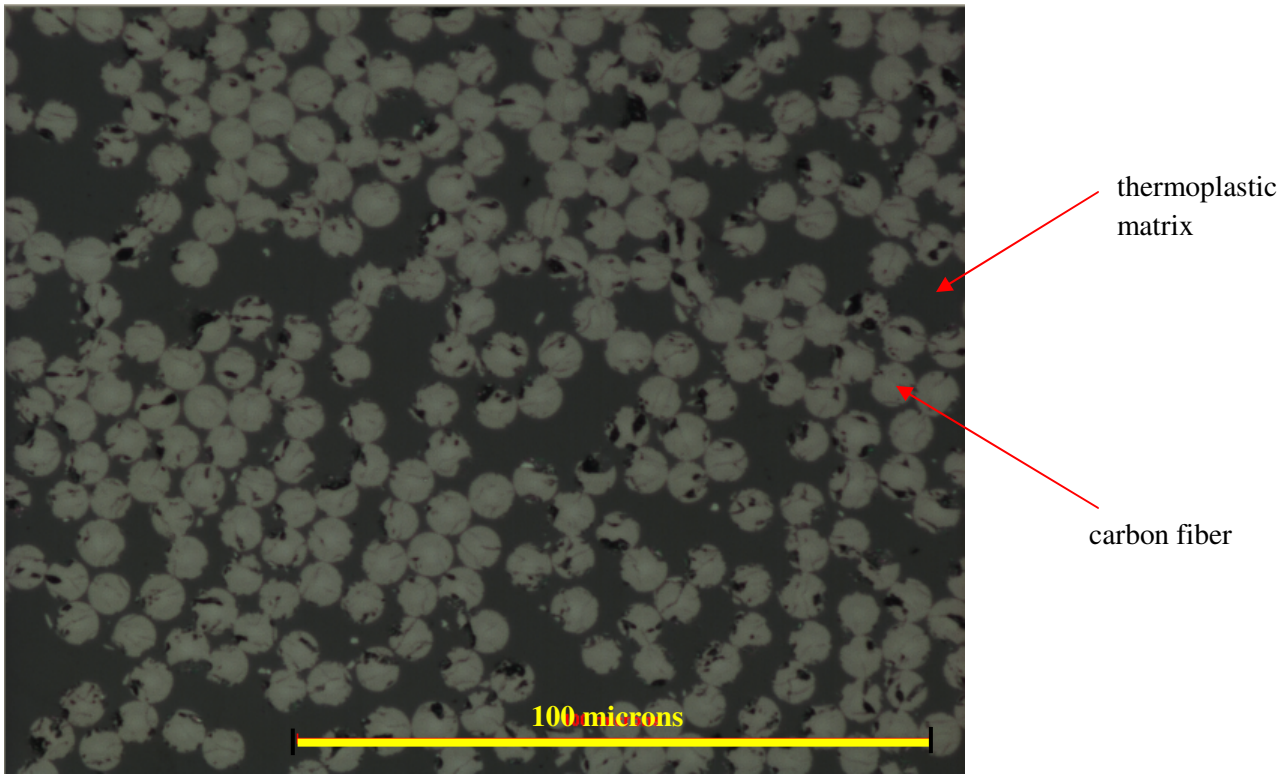

Figure 43: 500x micrograph of cross section of TP 4 shows even resin distribution.

The micrographs of these composite samples show no significant visual distinction between the stronger and weaker materials. There is some variation in the resin distribution between materials however it is not related to which materials are stronger or weaker and could be just because of where on the composite the image was taken.

Discussion

Mechanical Testing

The mechanical testing showed a correlation between flexural strength and tensile strength. The average values from each test graphed against each other gave R^2 values above 0.98 and there were no outliers in the data. The only discrepancy that did happen with these data sets was the overlapping of values for materials TP 1 and TP 2. For the 3 point bend test this overlap in values led to the mean of TP 2 being a higher stress value than the mean of TP 1. To verify that this did not invalidate the data a statistical analysis was run using a STAT 17 program (**Figure 26**).

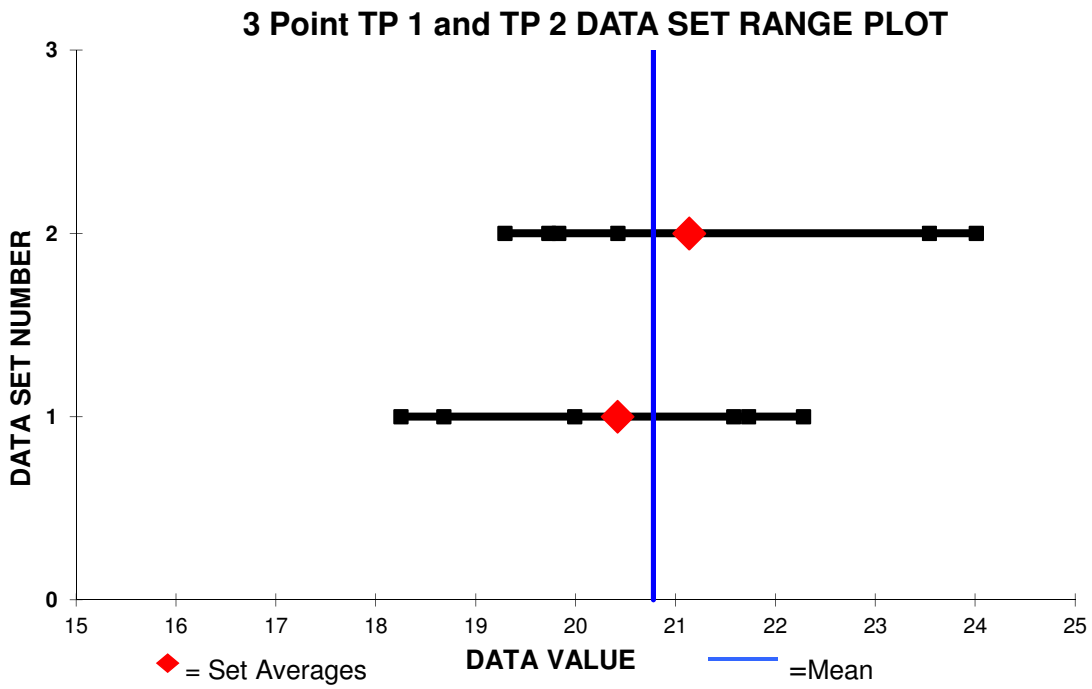

Figure 44 shows the 3 point bend test data ranges for TP 1 and TP 2 and how closely they overlap and correlate.

Figure 44 provides a visual of the overlap of data ranges for TP 1 and TP 2 with their means highlighted in red. The STAT 17 program also performed an Anderson-Darling Test that confirmed these two data sets were from the same population. An Equality of Variances Test was also done and established that the variances were equal. These statistical tests are scientifically accepted results that prove the insignificance of the mean of TP 2 being higher than the mean TP 1 value for the 3 point flexural tests. The data sets are comparable and the important factor to note is the gap between stress values of the first two thermoplastic resin system composites and the second two.

This project was a good start in data collection for TenCate's desire to replace tensile testing with bend testing for qualification of materials. The graphs of each individual material show small ranges (no more than 6ksi) in flexural and tensile strength values. This study was worthwhile and should continue

but more samples and variables need to be introduced before qualification using bend testing can be officially approved.

SEM Images

The SEM images verified the hypothesis that the drop in strength of these composites is directly related to the strength of the bond between the fibers and their matrix. There is an apparent difference between the wetting of the fibers by TP 1 2 and the wetting of the fibers done by TP 3 and 4. This lack of consistency in adhesion could be a result of two different thermoplastic matrices. Based on the strength values provided by CES being so similar, it is difficult to decipher which of these samples have which thermoplastic resin system. It was however revealed by TenCate that at least some of the resin systems were PEEK based. Looking at the flexural and tensile strength values provided by CES, PEEK is one of the higher strength resin systems and is most likely the base resin system in TP 1 and TP 2. PPS on the other hand, has the lowest flexural and tensile strength values and could be the base thermoplastic resin in TP 3 and TP 4.

It is important to remember that the strength values provided in **Table I** are based on thermoplastic matrices with 30% fiber volume fraction while the samples used in this project had 60% fiber volume fraction. Although the values will be different, the strength of the fiber reinforced thermoplastic is still based on the strength of the Van der Waals bond between the fiber and matrix and therefore the trend of strengths remains the same. A fiber-reinforced thermoplastic with lower strength with a 30% fiber volume fraction will also have the lower strength with a 60% fiber volume fraction.

The slight differences in strength between TP 1 and 2 and TP 3 and 4 are most likely due to variances in processing rather than resin systems. Both the flexural and strength values in these data sets are too similar to be caused by different thermoplastic resin systems all together.

Micrographs

The micrographs taken in this project did not show any differences in microstructure that related to the differences in strengths of the materials. All of the materials had sections with even resin distributions and other sections with uneven resin distribution. All of the materials also had black residue remaining after the polishing process. The residue is found along the fiber boundaries which could be explained by cracks in the fiber-matrix interface. If this experiment was to continue and there was time to take micrographs of more materials that could yield different results. Also further analysis could reveal the reason for the residue and/or what it is.

Conclusions

1. The average tensile strengths of TP 1 is 13.03 ksi, TP 2 is 12.43 ksi, TP 3 is 6.01 ksi, and TP 4 is 4.35 ksi
2. The average 3 point flexural strengths for TP 1 is 20.42 ksi, TP is 21.14 ksi, TP 3 is 10.65 ksi, and TP 4 is 7.55 ksi.
3. The average 4 point flexural strengths for TP 1 is 18.34 ksi, TP 2 is 16.80 ksi, TP 3 is 7.99 ksi, and TP 4 is 5.35 ksi.
4. There is a direct correlation between the 90 degree flexural strength and 90 degree tensile strength of carbon fiber reinforced thermoplastic composites with an R^2 value > 0.98

5. Poor fiber-matrix bonds decrease the strength of carbon fiber reinforced thermoplastic composites.
6. Resin distribution does not change between the two thermoplastic matrices tested in this report.

References

1.Mallick, P.K. Aircraft and Military Applications. *Fiber-Reinforced Composites: Materials, Manufacturing, and Design.* Boca Raton : Taylor & Francis Group, 2008.

2. Hale, Justin. Boeing 787 From the Ground Up. *The Boeing Company.* [Online] [Cited: January 21, 2012.] http://www.boeing.com/commercial/aeromagazine/articles/qtr_4_06/article_04_1.html.

3. The Boeing Company. Boeing. [Online] January 2012. [Cited: January 29, 2012.] http://www.boeing.com/companyoffices/aboutus/.

4. Hedge, Raghavendra R., Atul Dahiya, and M. G. Kamath. "Carbon Fibers." *University of Tennessee, Knoxville*. Apr. 2004. Web. 20 May 2012. <http://www.engr.utk.edu/mse/Textiles/CARBON%20FIBERS.htm>.

5. "Basics of Design Engineering - Engineering Materials - Plastics and Properties - Thermoplastic Composites." *Basics of Design Engineering - Engineering Materials - Plastics and Properties - Thermoplastic Composites*. Web. 5 May 2012. <http://machinedesign.com/BDE/materials/bdemat3/bdemat3_1.html>.

6. Schwartz, Mel M. *Composite Materials Handbook*. New York: McGraw-Hill, 1992. Print.

7. Solaimurugan, S., and R. Velmurugan. "Influence of In-plane Fibre Orientation on Mode I Interlaminar Fracture Toughness of Stitched Glass/polyester Composites." *Science Direct*. Web. 5 May 2012. <http://www.sciencedirect.com/science/article/pii/S026635380800033X>.

8. ASTM Standard D790-03, 2003, "Standard Tests Methods for Flexural Properties of Unreinforced and Reinforced Plastics and Electrical Insulating Materials", ASTM International, West Conshohocken PA, 2003.

9. CES EduPack. Vers. 6.2.0. Cambridge: Granta Designed Limited, 2012. computer software.

10. "Module 2: The Tensile Test." *Module 2: The Tensile Test*. Web. 15 May 2012. <http://dolbow.cee.duke.edu/TENSILE/>.

11. "Unidirectional Composite Axial Tensile Specimens : Composites World." *Unidirectional Composite Axial Tensile Specimens : Composites World*. Web. 15 May 2012. <http://www.compositesworld.com/articles/unidirectional-composite-axial-tensile-specimens>.

12. "Microscopy of Composites." *Welsh Composite Centre*. Welsh Composites Company, 16 Jan. 2011. Web. 15 May 2012. <http://welshcomposites.co.uk/downloads/Microscopy%20Webinar.pdf>.

13. ABET Criteria for Accrediting Engineering Programs, 2012-2013, www.abet.org/engineering-criteria-2012-2013.

14. ASTM Standard D 3039-00, 2000, "Standard Test Method for Tensile Properties of Polymer Matrix Composite Materials", ASTM International, West Conshohocken PA, 2000.

15. ASTM Standard D 6272-02, 2002, "Standard Test Method for Flexural Properties of Unreinforced and Reinforced Plastics and Electrical Insulating Materials by Four-Point Bending", ASTM International, West Conshohocken PA, 2002.

16. *Failure Analysis: Rough Grinding and Polishing (ASM Handbook,* Volume 21, 2003).